HHS Public Access

Author manuscript

Nat Microbiol. Author manuscript; available in PMC 2021 February 28.

Published in final edited form as:

Nat Microbiol. 2020 December ; 5(12): 1532–1541. doi:10.1038/s41564-020-0781-2.

Fluoxazolevir inhibits hepatitis C virus infection in humanized chimeric mice by blocking viral membrane fusion

Christopher D. Ma[1], **Michio Imamura**[2], **Daniel C. Talley**[3], **Adam Rolt**[1], **Xin Xu**[3], **Amy Q. Wang**[3], **Derek Le**[1], **Takuro Uchida**[2], **Mitsutaka Osawa**[2], **Yuji Teraoka**[2], **Kelin Li**[4], **Xin Hu**[3], **Seung Bum Park**[1], **Nishanth Chalasani**[1], **Parker H. Irvin**[1], **Andres E. Dulcey**[3], **Noel Southall**[3], **Juan J. Marugan**[3], **Zongyi Hu**[1], **Kazuaki Chayama**[2], **Kevin J. Frankowski**[4], **T. Jake Liang**[1]

[1]Liver Diseases Branch, NIDDK, NIH, Bethesda, MD, USA

[2]Department of Gastroenterology and Metabolism, Graduate School of Biomedical & Health Science, Hiroshima University, Hiroshima, Japan

[3]Chemical Genomics Center, Division of Preclinical Innovation, NCATS, NIH, Rockville, MD, USA

[4]Center for Integrative Chemical Biology and Drug Discovery, UNC Eshelman School of Pharmacy, Chapel Hill, NC, USA

Abstract

Fluoxazolevir is an aryloxazole-based entry inhibitor of hepatitis C virus (HCV). We show that fluoxazolevir inhibits fusion of HCV with hepatic cells by binding HCV envelope protein 1 (E1) to prevent fusion. 9 of 10 fluoxazolevir-resistance-associated substitutions are in the E1 protein and 4 are in a putative fusion peptide. Pharmacokinetic studies in mice, rats and dogs revealed that fluoxazolevir localizes to the liver. A four-week intraperitoneal regimen of fluoxazolevir in humanized chimeric mice infected with HCV genotype 1b, 2a or 3 resulted in a 2-log reduction in viremia, without evidence of drug resistance. In comparison, daclatasvir, an approved HCV drug, suppressed more than 3-log of viremia but is associated with emergence of resistance-associated substitutions in mice. Combination therapy using fluoxazolevir and daclatasvir cleared HCV genotypes 1b and 3 in mice. Fluoxazolevir combined with glecaprevir and pibrentasvir was also effective in clearing multidrug-resistant HCV replication in mice. Fluoxazolevir may be promising as the next generation of combination drug cocktails for HCV treatment.

Address correspondence and reprint requests to: T. Jake Liang, M.D., Liver Diseases Branch, National Institute of Diabetes and Digestive and Kidney Diseases, National Institutes of Health, Bethesda, Maryland 20892, USA, jliang@nih.gov.

Author contributions

T.J.L., C.D.M., Z.H. and K.J.F. conceptualized and designed the study. C.D.M., M.I., D.C.T., A.R., X.X., A.Q.W., D.L., T.U., M.O., Y.T., K.L., X.H., S.B.P., N.C., P.H.I., A.E.D., N.S., J.J.M., Z.H., K.C. and K.J.F. performed, analyzed and contributed to all the experiments. C.D.M., Z.H. and T.J.L. wrote the manuscript. All other authors reviewed and contributed to the manuscript.

Competing interests: The authors have no competing conflicts of interest to report.

Introduction

Hepatitis C virus (HCV) is a positive-sense, single-stranded, 9.6-kb virus in the *Flaviviridae* family that infects over 70 million people worldwide[1]. HCV is one of the leading causes of liver cirrhosis, hepatocellular carcinoma and liver failure[2]. Once exposed to the virus, patients may remain asymptomatic for months, impeding the treatment-seeking process[3]. Since interferon was first tested in the 1980s, the cure rate of HCV has steadily improved with the development of direct-acting antivirals (DAAs)[4,5]. A combination of first-generation DAAs with pegylated interferon-α and ribavirin was first approved in 2011, elevating the cure rate to nearly 90% from about 50% with just peginterferon and ribavirin[4,5]. Current DAA combination regimens are more effective with fewer side effects and have a higher barrier to drug resistance, improving the sustained virologic response (SVR) rate to more than 90%[4,5].

Despite this progress, there are still areas of unmet needs in HCV therapy. Many HCV-infected individuals do not have access to existing treatments because of high costs[6]. Also, DAA therapy is less effective in difficult-to-treat patients such as genotype 3 HCV infection with or without cirrhosis[7]. New and unusual subtypes (non-1a/1b, 3b, 4r, etc.) have also been discovered in patients from Asia and Africa, and are less responsive to the current pan-genotypic regimen, sofosbuvir/velpatasvir, with a 50% SVR[8–10]. DAAs and other commonly used drugs confer undesirable side effects and drug-drug interactions[11]. Many current treatment durations are lengthy at 12–24 weeks, though, in some cases, 8 weeks may suffice[12]. Shorter treatment durations may reduce costs and improve compliance. Finally, the emergence and transmission of HCV strains with multidrug resistance-associated substitutions (RASs) are a growing concern since they are less responsive to DAA retreatment[13–15]. In some studies, the response to retreatment is lower than 50% due to these multidrug RASs[14]. HCV reinfection occurs invariably in the transplant setting and effective preventive treatment, such as the use of HBIG in preventing HBV reinfection after liver transplant, would be valuable[16]. New antivirals are therefore needed to improve treatment efficacy and shorten its duration.

We previously identified a promising aryloxazole-based series of HCV entry inhibitors, which have a structural scaffold different from other described HCV entry inhibitors[17]. After further structure-activity relationship optimization, we identified the compound 18a (NCGC00351982 or fluoxazolevir), as the lead candidate for preclinical development based on the best combined profile of efficacy, cytotoxicity and *in vitro* ADME (EC_{50}=0.0188 μM, CC_{50}=13.0 μM, selectivity index CC_{50}/EC_{50}>600)[18]. We report here the mechanism of action of fluoxazolevir, including *in vitro* efficacy against various HCV genotypes, synergy with other currently FDA-approved HCV drugs, *in vivo* pharmacokinetics in mice, rats and dogs, and efficacy in a humanized chimeric mouse model against HCV genotype 1b, 2a or 3 infection.

Results

Fluoxazolevir inhibits HCV fusion with hepatic cells

In a previous study, fluoxazolevir (Fig. 1a) was shown to target the entry step of the HCV life cycle using a HCV pseudoparticle assay[18]. To confirm fluoxazolevir's role in inhibiting HCV entry, a time-of-addition assay was performed[19]. Bafilomycin A1, a vacuolar-type H^+-ATPase inhibitor, (*S*)-CCZ, a previously identified HCV late entry inhibitor[19], and sofosbuvir, a NS5B polymerase inhibitor, were used as controls. Overall, fluoxazolevir showed a similar pattern of HCV inhibition to that of (*S*)-CCZ (Fig. 1b). Both fluoxazolevir and (*S*)-CCZ displayed potent inhibition similar to the continuous treatment when added either simultaneously or 2 h prior to infection. When fluoxazolevir and (*S*)-CCZ were administered 1 hour after infection, both compounds were still effective in inhibiting infection. Bafilomycin A1 behaved similarly but when added either 2 h before or 1 h after infection, it was much less effective, suggesting a more transient effect. In contrast, sofosbuvir was completely ineffective when the treatment was administered 2 h prior to infection but very potent when added simultaneously or any time after infection. The time-of-addition assay confirmed that fluoxazolevir targets the entry stage of the HCV life cycle.

A membrane fusion assay was performed to define whether fluoxazolevir targets viral fusion or another viral entry step (Fig. 1c)[20]. To prevent premature endosomal acidification, and consequently HCV entry, 10 mM NH_4Cl was added in all solutions throughout the assay[21]. Cell receptor binding was synchronized when high-titer HCV with NH_4Cl was added to cells for 3 h at 4°C[22]. Forced HCV internalization and fusion with cytosolic lysosomes were then triggered by changing the overall pH of the medium to pH 5 for 5 minutes. Following the pH shift, cells were incubated at 37°C for 3 h, washed, cultured in regular media without NH_4Cl for 72 h and then analyzed for infection rate.

In the fusion assay (Fig. 1c & 1d), compounds were added at various times to test for specificity in inhibiting viral fusion. In protocols I and II, bafilomycin A1 behaved similarly to the DMSO control treatment. As expected, the artificial lowering of the cytosolic pH overcame the block of endosomal acidification by bafilomycin A1, thus allowing HCV fusion to occur[22]. In contrast, HCV infection only increased minimally by 1.6-fold after the pH shift in the fluoxazolevir-treatment group, which was significantly lower than those of the DMSO (6.5-fold) and bafilomycin A1 (3.5-fold) groups. This finding indicates that fluoxazolevir blocks viral fusion within the endosomes even under an acidic environment. In protocol III, both fluoxazolevir and bafilomycin A1 failed to inhibit HCV infection since the compounds were added after the viral fusion step. Altogether, fluoxazolevir specifically inhibits the fusion step of HCV entry.

Fluoxazolevir binds to HCV E1 protein

To further support that fluoxazolevir targets the E1 protein, a fluoxazolevir-diazirine-biotin (fluoxazolevir-DB) probe was synthesized (Extended Data Fig. 1a). Fluoxazolevir-DB showed inhibition against HCV infection in a dose-dependent manner with an EC_{50} of 1.19 μM (Extended Data Fig. 1b), and was stable at room temperature and under ambient light with slow decomposition after a few days (Extended Data Fig. 1c & d). When performing

the fluoxazolevir-DB cross-linking experiment with recombinant HCV E1/E2 proteins under UV-irradiation, the activated cross-linked product was identified to be the E1 protein by Western blot with anti-E1 antibody (Fig. 1e). Under various control conditions, such as fluoxazolevir-DB without UV activation, DMSO, and a sample with excess fluoxazolevir (200 μM) to compete against fluoxazolevir-DB (2 μM), the E1 protein was not detected. A similar UV cross-linking experiment was performed with fluoxazolevir-DB (5 μM) and Huh7.5.1 cells infected with high-titer chimeric genotype 1a HCV and showed specific cross-linking of fluoxazolevir-DB to E1 (Fig. 1f).

Fluoxazolevir resistance-associated substitutions in E1

To further study the mechanism of action and genetic barrier to drug resistance of fluoxazolevir, an *in vitro* drug-induced resistance selection assay was performed[23]. Fluoxazolevir resistance emerged after 21 passages (Supp. Fig. 1) compared to 11 passages for NS5A inhibitor daclatasvir (Supp. Fig. 2), indicating that fluoxazolevir may have a higher genetic barrier to resistance than daclatasvir. Amplified viruses from some of these passages (wells A1, B1, C1, E1, G1 and H1) showed a significant shift of fluoxazolevir dose-response curves (an increase of EC_{50} >2-fold), indicating the generation of the fluoxazolevir RASs (Extended Data Fig. 2). It is not clear why amplified viruses from other passages (wells D1 and F1) did not show any significant resistance to fluoxazolevir. It is possible that certain RASs may have been less fit and promptly revert to the wild-type sequence in the final amplification passage, in which the compound was not added. Sequencing of the core, E1 and E2 regions of the viral isolates at the last stage of each selection passage identified various potential RASs (Fig. 2a & 2b), which were validated in the amplified viral stock. In the selection assay with daclatasvir (Supp. Fig. 2), a common RAS (NS5A F28C) was found[15,24], supporting the validity of this assay.

Mutations were then introduced individually into the HCV wild-type genome to confirm their resistance against fluoxazolevir. The mutant viral clones replicated similarly (no more than 20% difference) to the HCV wild-type clone (Extended Data Fig. 3a & 3b). Analysis of infectious virus production in the culture supernatant showed that most RAS-containing viruses produced similar levels of infectious virus in comparison to the HCV wild-type except for two E2 mutants: M405V and P616A, which produced somewhat lower infectious viral titers, and V414A, which produced more infectious virus (Extended Data Fig. 3a & 3c). The E1 RASs showed minor to moderate resistance (Fig. 2c & 2d, Extended Data Fig. 4). Among them, A274S, I374T, D382E and V414A exhibited notable resistance with the EC_{50}'s shifting from 36.7 nM against the HCV wild-type to 201 nM, 242 nM, 169 nM and 176 nM, respectively. Many of the mutations clustered in the E1 fusion peptide sequence, supporting the concept that fluoxazolevir targets the HCV fusion process. Two E1 mutations (I374T and D382E) occurred outside the fusion peptide and showed resistance (Fig. 2c). Mutations in the E2 protein (T395A, M405V, P616A) were also detected but they all occurred in the presence of validated resistant E1 mutations, and when tested individually, they did not show much resistance (Fig. 2c, Extended Data Fig. 4).

Fluoxazolevir inhibits HCV chimeric infection

Dose-response assays of fluoxazolevir were performed against all chimeric HCV-RLuc genotypes including 1a, 1b, 2b, 3a, 4a, 5a, 6a and 7a (Fig. 3)[25] and compared to the wild-type, J6/JFH1 HCV-RLuc (genotype 2a). Fluoxazolevir was generally effective against all HCV genotypes and reached a maximum inhibition close to 100% at concentrations below significant toxicity. Fluoxazolevir did show genotypic variations in efficacy with varying EC_{50} values. It was most effective against HCV 2a and 2b, followed by 3a and 6a, all within sub-μM EC_{50} values. Fluoxazolevir also displayed little to no cytotoxicity, with CC_{50} > 20 μM in primary human hepatocytes, MT-4 cells, HepG2 cells and peripheral blood mononuclear cells (Extended Data Fig. 5), and ~12 μM in Huh7.5.1 cells (Fig. 3).

Fluoxazolevir synergizes with other anti-HCV drugs

To explore the potential combination of fluoxazolevir with currently available anti-HCV drugs, we tested the synergistic antiviral effects of fluoxazolevir with human interferon-α, ribavirin, daclatasvir, sofosbuvir and simeprevir (NS3/4A protease inhibitor). Two commonly used programs to calculate synergy, CalcuSyn and MacSynergy II, were applied[26]. CalcuSyn calculates combination indices by analyzing the inhibitory effects near the EC_{50} values for each drug[27], while MacSynergy II utilizes the Bliss independence model[28]. Both programs use different definitions to determine the level of synergy, thus each program provides a different but complementary profile of synergistic analysis. Drug combinations were added in a dose-dependent manner to determine whether the inhibitory effects of the treatment were synergistic, additive, equal or antagonistic to the inhibitory effects of each drug independently. CalcuSyn showed that fluoxazolevir was highly synergistic with all five selected antivirals while MacSynergy II provided varying extents of synergism (Table 1).

Pharmacokinetic and toxicity studies in animal models

After single-dose administration in mice and rats, fluoxazolevir showed preferential localization in the liver with long $t_{1/2}$ values for both IV and PO routes: 17–37 h in the plasma and 26–45 h in the liver (Extended Data Fig. 6a & 6b, Extended Data Fig. 7). When fluoxazolevir was administered intravenously (3 mg/kg), the volume of distribution at steady-state (V_{dss}) was 137 L/kg and 12±3 L/kg for CD-1 mice and SD rats, respectively. The high values of V_{dss} suggested that the compound penetrated tissues extensively. After PO administration (10 mg/kg), the C_{max} values in the plasma were 0.084 μM and 0.017 μM, the C_{max} values in the liver were 34.4 μM and 39.9 μM, and the liver to plasma AUC ratios were 659 and 6250 for CD-1 mice and SD rats, respectively (Extended Data Fig. 7). The oral bioavailabilities were 37% and 1.2 % for CD-1 mice and SD rats, respectively, after a 10 mg/kg PO administration (Table 2).

In dogs, fluoxazolevir exhibited a similar pharmacokinetic profile as in the rodents (Table 2 & Extended Data Fig. 6c), with a long $t_{1/2}$ via IV (3 mg/kg dose; 29 h) and PO (10 mg/kg dose; 19 h), high plasma clearance (67±6 mL/min/kg), large V_{dss} (144±15 L/kg) and bioavailability of 14%. Analysis of urine samples collected for 10 days after the IV dosing showed a total renal excretion of 2.3±0.4%.

A single dose of fluoxazolevir in these animals did not show any evidence of liver injury (ALT elevation) or other notable toxicity (Extended Data Fig. 6d). Maximum tolerable dose in CD-1 mice was determined by administering a single dose of 50, 100, 500 or 1000 mg/kg fluoxazolevir by oral gavage with daily assessment of toxicity (body weight, observation, mortality and necropsy) for 3 days (Extended Data Fig. 8). No evidence of toxicity at any of those doses was observed.

Fluoxazolevir suppresses HCV infection in humanized chimeric mice

The antiviral effect of fluoxazolevir was tested in human hepatocyte-engrafted *Alb-uPA/Scid* chimeric mouse models infected with HCV genotypes 1b, 2a or 3. Fluoxazolevir was administered intraperitoneally daily for 4 weeks in two dosing groups for genotypes 1b and 2a (0.1 mg/kg and 1 mg/kg) and one dosing group for genotype 3 (5 mg/kg), and the animals were followed off-treatment for an additional 4 weeks. During treatment, viral RNA levels steadily declined for all genotype infections treated with fluoxazolevir (Fig. 4a, Supp. Fig. 3), as compared to the untreated mice. The 1 mg/kg dose was more effective in the genotype 1b-infected mice, which decreased the viral RNA titer by about 2-log, than in the genotype 2a-infected mice, which decreased the viral titer by about 1-log. The 5 mg/kg dosage for genotype 3-infected mice had a decrease in viral RNA titer by approximately 1.5-log (Fig. 4b, Supp. Fig. 4–5). Throughout the course of treatment, there was no evidence of viral rebound, but RNA levels rebounded after the treatment ended. No RASs were identified after sequencing the virus before and after treatment, suggesting a high barrier of drug resistance *in vivo* (Supp. Table 1). Finally, there was no evidence of toxicity during the course of treatment (Extended Data Fig. 9).

Fluoxazolevir and daclatasvir combination therapy

Based on the synergy results and the demonstrated antiviral effects of fluoxazolevir *in vivo*, a four-week combination therapy of fluoxazolevir and daclatasvir was conducted in humanized *Alb-uPA/Scid* mice infected with HCV genotype 1b or 3 to evaluate whether a SVR can be achieved. Monotherapy with daclatasvir was performed in comparison. The doses administered for fluoxazolevir and daclatasvir were 5 mg/kg IP daily and 10 mg/kg PO daily, respectively. In combination treatment of both genotype-infected mice, the viral RNA levels in the serum rapidly decreased to undetectable levels without any evidence of emerging drug resistance and remained undetectable 4 weeks after stopping treatment, consistent with a SVR (Fig. 4b). On the other hand, daclatasvir monotherapy caused a rapid decline in viral levels, but the viremia either never reached undetectable levels or rebounded, likely a result of emerging RASs. This study demonstrates that fluoxazolevir in combination with a DAA can achieve SVR against different HCV genotypes.

Human serum albumin levels were measured to monitor the engrafted human hepatocytes in all mice. During the entire course of treatment and follow-up, the human serum albumin levels remained relatively constant (Fig. 4a–d, Supp. Fig. 3–5, Extended Data Fig. 10), indicating that the reduction of HCV RNA was not caused by a loss of engrafted hepatocytes. One mouse from each treatment group infected by HCV genotype 1b showed a gradual decline of human serum albumin with time (Supp. Fig. 4).

Fluoxazolevir is active against multidrug-resistant HCV

Mavyret, a combination of glecaprevir (GLE, a NS3/4A inhibitor) and pibrentasvir (PIB, a NS5A inhibitor), is a second-generation DAA regimen that is active against all HCV genotypes *in vitro* and *in vivo*, and shows little or no loss of efficacy in common RASs reported[29–31]. Despite its high clinical efficacy, drug-resistant variants have been reported[32]. An HCV genotype 1b strain resistant to GLE/PIB had been generated in humanized chimeric mice infected with HCV genotype 1b by serial treatment with GLE/PIB[33]. The virus contains NS3-D168E, a well-known NS3/4A RAS[30], and multiple NS5A RASs (Q24R, R30E, P58S and A92K). Humanized chimeric mice infected with this virus respond poorly to GLE/PIB treatment; interestingly, the RASs persist in the mice despite the absence of treatment[33]. The NS5A-P58S has been reported in Mavyret-treated HCV patients with relapse[32]. The NS5A-R30E has not been reported but other RASs affecting this residue are known[31,34].

A six-week combination therapy with fluoxazolevir and GLE/PIB was conducted in humanized chimeric mice infected with this multidrug-resistant HCV strain. Fluoxazolevir was administered at a daily dose of 5 mg/kg while GLE and PIB were administered at a daily dose of 60 mg/kg and 24 mg/kg, respectively. In addition, fluoxazolevir or GLE/PIB was administered separately as monotherapy groups. Another group of infected mice was untreated and monitored for viremia, which showed steady levels during follow-up (Extended Data Fig. 10a). Fluoxazolevir-treated mice showed a 1–2 log gradual decline of HCV viremia (Fig. 4c, upper panel), similar to what was observed in mice infected with HCV wild-type genotype 1b, 2a or 3. In GLE/PIB-treated mice, HCV viremia declined 2–5 logs but never reached an undetectable level, except for one time point in mouse HSB0190–0037 (Fig. 4c, middle panel). All mice rebounded to pre-treatment viremia levels after fluoxazolevir or GLE/PIB was stopped. In combination-treated mice, HCV RNA decreased rapidly to undetectable levels and remained below detectable levels throughout the duration of treatment, indicating the effectiveness of fluoxazolevir together with GLE/PIB in suppressing this multidrug-resistant variant (Fig 4c, lower panel, Extended Data Fig. 10b). After stopping treatment, all three surviving mice continued to show undetectable levels of HCV RNA for a week. With a longer follow-up of 4 weeks, one mouse died, one showed a viral rebound, and the third continued to have an undetectable level of HCV RNA. Sequence analysis of the virus in the mouse with post-treatment relapse showed the same drug-resistant substitutions in NS3 and 5A as the inoculum virus (Supp. Table 1).

Acute HCV infection is delayed by fluoxazolevir

Since fluoxazolevir targets viral entry, it may potentially serve as an HCV preventive treatment. To determine the effectiveness of fluoxazolevir as a preventive therapy for HCV infection, a 1 mg/kg daily treatment was administered intraperitoneally for five days before and two weeks after HCV genotype 1b inoculation (Fig. 4d, Supp. Fig. 6). In the control group without treatment, viral RNA levels increased to about 6-log a week after infection while the viral RNA levels for the pretreated group gradually increased only to about 3-log. After stopping treatment, the HCV RNA levels steadily increased for both groups; however, the viral RNA levels for the preventive group were still significantly lower than those of the

control group. This data suggests that an entry inhibitor, such as fluoxazolevir, can partially prevent and hinder the progression of HCV infection *in vivo*.

Discussion

In generating fluoxazolevir-resistant HCV clones, we identified multiple mutations in the putative E1 fusion loop, a sequence spanning between amino acids 264 and 290[35,36], that confer drug resistance to fluoxazolevir. Two of the mutations have been induced by (S)-CCZ, another HCV fusion inhibitor (M267V and F291L)[37], but the other RASs are unique to fluoxazolevir (A274S and F291V). Therefore, selection of fluoxazolevir-resistant substitutions in the fusion peptide of E1 shows that fluoxazolevir blocks HCV entry by interrupting the viral fusion process. Fluoxazolevir-DB also binds directly to E1 through UV-activated cross-linking, which further supports that it interacts with E1 to prevent viral entry. Two E1 RASs (I374T and D382E) outside the fusion peptide in the distal transmembrane domain, potentially playing a role in anchoring the transmembrane domain to the plasma membrane and the fusion process[38,39]. Both mutants also showed lower viral fitness in comparison to the wild-type, likely due to a disruption of structural integrity in this hydrophobic domain[40].

E2 interacts closely with E1 as a heterodimer[39] and may play a role in the fusion process[41] in addition to its interaction with host entry factors. Thus, E2 mutations may contribute to resistance against fluoxazolevir. F345V/V414A mutations in HCV genotype 3a (S52 strain) have been reported to enhance the release of infectious virus particles and confer resistance against interferon-α[42]. Increased viral fitness could account for the apparent drug resistance against the V414A mutant. Analyses of the replicating and infectious capacities of the described mutants show that many of them are less infectious than the wild-type, suggesting that these RASs are less fit and may not persist once the drug is removed.

Fluoxazolevir can achieve complete inhibition against all 7 HCV chimeric genotypes *in vitro* with varying efficacies. Fluoxazolevir is most active against HCV genotypes 2a and 2b, which is not unexpected as HCV genotype 2a was used to discover fluoxazolevir[18]. The *in vivo* studies in which fluoxazolevir is effective against genotypes 1b, 2a and 3 without the emergence of RASs support the broad genotypic coverage of fluoxazolevir. The pharmacokinetic studies demonstrated a favorable profile with high liver concentrations, long $t_{1/2}$ and reasonable oral bioavailability. With the dose administered, it was possible to achieve drug concentrations (>10 μM) in the liver that is substantially higher than the EC_{50}'s against all HCV genotypes without substantial toxicity.

Efficacy studies in humanized *Alb-uPA/Scid* mice showed that fluoxazolevir significantly suppressed HCV RNA levels during either monotherapy or combination therapy with daclatasvir. In mice infected with HCV genotypes 1b, 2a and 3, fluoxazolevir monotherapy decreased viral RNA significantly with no evidence of viral RNA rebound or generation of RASs. Daclatasvir monotherapy showed a greater decline in viral levels initially, which rebounded later during treatment, suggesting the emergence of RASs. In genotype 1b or 3-infected mice treated with a combination of fluoxazolevir and daclatasvir, viral RNA levels were mostly below the detectable limit throughout the entire treatment period and 4 weeks

after stopping treatment. Some of the post-treatments showed a detectable but not quantifiable HCV viremia at some points after stopping treatment, which may represent residual non-infectious viral genomes after clearance as it does not lead to rebound.

A potent entry inhibitor, especially in combination with other DAAs, can minimize resistance and shorten treatment duration. Recent development of an entry inhibitor, myrcludex B, against chronic hepatitis D[43], is a case in point for this therapeutic strategy. Entry inhibitors may also potentially prevent or delay HCV graft reinfection in liver transplantation. Recent use of HCV-positive organs in HCV-negative recipients has presented a unique opportunity for preemptive therapy with DAAs to prevent infection[44,45]. Fluoxazolevir potentially could be used at a higher dose or in combination with another DAA for this purpose.

In summary, we show that fluoxazolevir inhibits HCV entry by blocking membrane fusion of viral endosomes, which is also the mechanism of action for other recently described entry inhibitors, such as chlorcyclizine, flunarizine and 4-aminoquinoline derivatives[46–48]. Our preclinical studies support fluoxazolevir as a promising candidate for the next generation of drug cocktails for HCV treatment. It is synergistic with other FDA-approved HCV antivirals, active against all HCV genotypes *in vitro*, has preferential localization in the liver, can clear various HCV strains in a humanized mouse model, and has potential to delay or prevent acute HCV infection. As the viral fusion structure and process is relatively conserved[49], it is also tempting to speculate that fluoxazolevir may have more broad antiviral activities against other viruses.

Data availability

The data that were used to generate the HCV E1 alignment in Fig. 2b and to support the findings of this study are available from Virus Pathogen Resource database (genotypes 1–6). The two genotype 7 sequences are available in NCBI with the accession numbers YP_009272536 and ARB18146. Source data for Figs. 1b, 1d, 1e, 1f, 3, and 4, and Extended Data Figs. 1b, 2, 3b, 3c, and 4–10 are included in the article. Other data that support the findings of this study are available from the corresponding author upon request.

Methods

Cells, chemicals and viruses

HCV permissive cell line, Huh7.5.1, was maintained in DMEM (Thermo Fischer Scientific, Waltham, MA, USA) with 10% FBS and antibiotics in a 37°C and 5% CO_2 incubator. The cell lines were supplied from various sources: Huh7.5.1 cells, HepG2 cells, primary human hepatocytes (Thermo Fisher Scientific, Waltham, MA), MT-4 cells and peripheral blood mononuclear cells (NIH Department of Transfusion Medicine). All cell lines have been regularly checked for *Mycoplasma* using the MycoAlert Mycoplasma Detection Kit (Lonza, Morristown, NJ, USA) and confirmed to be *Mycoplasma*-free. None of the cells were authenticated but they have been used extensively in our laboratory and behaved as expected. Fluoxazolevir was synthesized at the Center for Integrative Chemical Biology and Drug Discovery, UNC Eshelman School of Pharmacy and fluoxazolevir-diazirine-biotin was

synthesized at the Chemical Genomics Center, National Center for Advancing Translational Sciences. (*S*)-CCZ was purified from racemic chlorcyclizine (CCZ, Sigma-Aldrich, St. Louis, MO, USA)[19]. HCV inhibitors were purchased from various commercial sources: bafilomycin A1 (Sigma-Aldrich, St. Louis, MO, USA), sofosbuvir (Advanced ChemBlocks Inc., Burlingame, CA, USA), ribavirin (Sigma-Aldrich, St. Louis, MO, USA), daclatasvir (Selleckchem, Houston, TX, USA), simeprevir (Selleckchem, Houston, TX, USA) and human interferon-alpha A (PBL Assay Science, Piscataway Township, NJ, USA). Wild-type HCV, HCV-RLuc (genotype 2a, J6-JFH1 clone) and various chimeric HCV-RLuc were generated according to the literature[25]. All constructs were confirmed via Sanger sequencing. HCV plasmids were linearized with XbaI (New England Biolabs, Ipswich, MA), transcribed with MEGAscript™ T7 Transcription kit (Thermo Fischer Scientific, Waltham, MA, USA) and electroporated into Huh7.5.1 cells with the Neon Transfection System at conditions of 1400 V, 20 ms and 1 pulse (Thermo Fischer Scientific, Waltham, MA, USA). The software program, Omega (Software Version: 1.10; Firmware Version: 1.21), was used to measure luminescence readings for all Renilla luciferase assays.

Time-of-addition assay

Huh7.5.1 cells were seeded in 96 well plates (10^4 cells per well) and cultured overnight. HCV-RLuc (genotype 2a) were used to infect cells with the treatment of fluoxazolevir (10 μM) at various treatment times (continuous, −2 h, 0 h, 1 h, 2 h and 3 h) as indicated in Fig. 1b. All treatments, except for the continuous group, were removed after 2 h of incubation and replaced with regular medium. Cells were further cultured for 48 h and then luminescence was assessed via the Renilla Luciferase assay system (Promega, Madison, WI, USA). DMSO (Sigma-Aldrich, St. Louis, MO, USA), (*S*)-CCZ (10 μM), bafilomycin A1 (10 nM) and sofosbuvir (10 μM) were used in parallel to fluoxazolevir as controls.

Membrane fusion assay

The assay was modified from a previous published method (Fig. 1c)[47]. Huh7.5.1 cells were seeded in 96-well plates coated with 0.01% polylysine (Sigma-Aldrich, St. Louis, MO, USA) (1.5×10^4 cells per well) and cultured overnight at 37°C. Cells were treated with NH_4Cl (10 mM) for 1 h at 37°C before infection of wild-type J6-JFH1 HCV (0.5 MOI) in the presence of NH_4Cl. Cells were incubated with the virus for 3 h at 4°C and washed gently with medium containing NH_4Cl. Cells were incubated for 5 min at 37°C with freshly prepared pH 5 or 7 citrate-phosphate buffer. Cells were incubated in medium containing NH_4Cl together with DMSO, 3 μM of fluoxazolevir, or 3 nM bafilomycin A1 in three protocols. In protocol I, the compound was added before the pH 5 shift and remains in solution until 3 h after the shift. In protocol II, the compound was added only during the pH shift. In protocol III, the compound was added after the pH shift and remains in the medium for 3 h. Cells were washed three times and cultured in regular DMEM for 72 h before being processed for HCV core immunofluorescent staining. HCV core-positive foci per well were recorded for the analysis of HCV infection under various conditions.

HCV core immunofluorescent staining

Huh7.5.1 cells were fixed with 4% paraformaldehyde diluted in phosphate-buffered saline (PBS) for 15 mins and then blocked with 3% w/v bovine serum albumin diluted in PBS with

0.3% v/v Tween-20. Anti-HCV core monoclonal antibody, which was generated from a 6G7 hybridoma clone and was generously provided by Drs. Harry Greenberg, was diluted in PBS by 1:500 v/v and was used as the primary antibody. Alexa Fluor 488 anti-mouse antibody (Thermo Fischer Scientific, Waltham, MA, USA) was diluted in PBS by 1:1000 v/v and was used as the secondary antibody. Cell nuclei was then stained with Hoechst dye (Thermo Fischer Scientific, Waltham, MA, USA). Quantification of HCV infection was measured via fluorescence microscopy.

UV-activated cross-linking and analysis of fluoxazolevir-diazirine-biotin and HCV E1 protein

The *in vivo* UV-activated cross-linking was performed by infecting Huh7.5.1 cells (3×10^6) with high-titer HCV genotype 1a in a 10-cm dish and subsequently adding fluoxazolevir-diazirine-biotin (fluoxazolevir-DB) (5 μM) or a control compound. The cells were incubated for 1 h at 37°C and the mixture was exposed to UV irradiation for photoaffinity cross-linking. The medium was removed, cells were washed twice with 5 mL of cold PBS and 1 mL of lysis buffer (30 mM Tris pH 7.5, 1 mM EDTA, 150 mM NaCl, 0.3% NP-40, 0.05% SDS) with a protease inhibitor cocktail was added. The cell lysate was pelleted via centrifugation at 20 K relative centrifugal force (rcf) at 4°C for 5 min. The supernatant was isolated and kept at 4°C prior to purification via Pierce NeutrAvidin agarose beads.

The Pierce NeutrAvidin agarose beads (Thermo Fischer Scientific, Waltham, MA, USA) were prepped before purification by spinning 50 μL of the beads down, discarding the supernatant and washing the beads with 1 mL of PBS twice. Biotin BSA (2 μL of 2 μg/mL biotin BSA in PBS) was added to the NeutrAvidin beads as a positive control. The cell lysate samples were then added to the beads, were briefly mixed, were placed on a rocker at 4°C for 1 h and were pelleted at 5000 rcf. The beads were then repeatedly washed twice with PBS followed by lysis buffer. After a final wash with PBS, elution buffer (2% SDS, 3 mM biotin, 6 M urea, 2 M thiourea)[50], 1:4 Laemmli buffer and reducing agent were added to the beads, were incubated for 10 min. at room temperature and then again for 10 min. at 95°C. Samples were then centrifuged and the supernatant was used for Western blot analysis via a ProteinSimple Wes capillary Western blot system (Wallingford, CT, USA). A4 anti-E1 antibodies (provided by Harry Greenberg, Stanford University, Palo Alto, USA) were used for the Western blot analysis.

In vitro drug-induced resistance selection assay

Huh7.5.1 cells were seeded in a black, clear bottom 96-well plate (10^4 cells per well), cultured overnight and then infected with wild-type J6/JFH1 HCV (1×10^5 ffu/mL) for 6 h to establish infection. After the incubation, the viral medium was replaced with 200 μL of DMEM containing various fluoxazolevir concentrations per column on the plate, increasing by two-fold from 10 nM to 5 μM (e.g., 5 μM in column 1, 2.5 μM in column 2, etc.). Columns 11 and 12 contained DMSO treatment (0.1% v/v) as a vehicle-only control. After 72 h, a two-part infection was performed: (1) reinfection under the same fluoxazolevir concentration and (2) challenge infection with a higher fluoxazolevir concentration (Supp. Fig. 1). For the first infection, 100 μL of virus-containing medium was transferred into another black, clear bottom 96-well plate seeded with uninfected Huh7.5.1 cells (10^4 cells

per well). Each well in this plate contained the same concentration as the wells in the original, infected plate. For the second infection, 50 μL of virus-containing medium was transferred to another black, clear bottom 96-well plate seeded with uninfected Huh7.5.1 cells and a two-fold higher fluoxazolevir concentration over the original well (e.g., a well containing 2.5 μM fluoxazolevir was passaged to a well containing 5 μM fluoxazolevir). The remaining 50 μL of the original virus-containing medium was stored at −80°C for further analyses. The part-one infected cells were analyzed via HCV core immunofluorescent staining to quantify productive infection for the previous passage. The two-part infection protocol was repeated every 3 days until positively infected cells were observed at 5 μM of fluoxazolevir. At this stage, the selected viral isolates were then amplified in the presence of fluoxazolevir to generate a stock for further analyses. The core, E1 and E2 regions of the viral isolates and their amplified viral stocks were sequenced (Fig. 2a). For the selection of daclatasvir-resistant variants, a concentration range of 10 pM to 5 nM was used.

In vivo pharmacokinetics

Male CD-1 mice and SD rats were obtained and were maintained at the NIH animal facilities where all protocols were followed by the Division of Veterinary Resources and the Animal Care and Use Committee at the NIH. The pharmacokinetic studies in male beagle dogs were conducted by the Charles River Laboratories (Worcester, MA) under their IACUC approved protocol (PS-0002-DA-DE). All mice, rats and dogs used in the pharmacokinetics studies were selected randomly and no animals were given preferential treatment when allocating them into the experimental groups. The sample size was chosen based on the minimal number needed for statistical analysis.

The dosing solution of fluoxazolevir was freshly prepared prior to the drug administration in 10% polyethylene glycol, 10% ethanol and 16% 2-hydroxypropyl-β-cyclodextrin (HPβCD) for IV and PO routes. The pharmacokinetic data were evaluated after a single dose at the stated route (i.e. oral gavage, IV injection). Blood, liver, brain and heart samples from the CD-1 mice, blood and liver samples from the SD rats, and blood and urine samples from the dogs were collected at various time points post-administration. Three samples (n=3) were collected at each time point. Collected samples were immediately frozen and stored at −80°C before analysis. Fluoxazolevir concentrations in the plasma, liver, brain, heart and urine were measured using ultraperformance liquid chromatography-mass spectrometry (UPLC-MS/MS). The pharmacokinetic parameters were presented as mean ± standard error of the mean (SEM) for rats (n=3, plasma) and dogs (n=3). Pharmacokinetic parameters were derived using noncompartmental method with Phoenix WinNonLin, Version 6.2.0 (Certara, St. Louis, MO, USA)[46].

In vivo efficacy studies in humanized chimeric mouse model

A humanized chimeric mouse model was used to test the efficacy of fluoxazolevir *in vivo* against HCV in three experimental formats: monotherapy, combination therapy with daclatasvir or Mavyret (glecaprevir/pibrentasvir), and preventive therapy. HCV infection was established by infecting human HCV serum samples containing either genotype 1b, 2a or 3, or mouse serum sample containing the multidrug-resistant HCV strain (10^5 HCV copies) in *Alb-uPA/Scid* mice engrafted with primary human hepatocytes provided by PhoenixBio Co.

Ltd (Hiroshima, Japan). Serum HCV RNA was monitored in the mice for 6 weeks before treatment. Serum HCV titers were monitored weekly in HCV-infected chimeric mice before and after treatment with various regimens of fluoxazolevir (IP). Human albumin levels in the mouse serum were measured in parallel to monitor the grafted human hepatocytes[46]. The experiments were conducted at Hiroshima University, Japan under approved animal protocols. All mice in the *in vivo* efficacy studies were selected randomly and were not given preferential treatment when allocating them into control or experimental groups. The sample size for each group was chosen based on availability of the animals at the time of the study.

Statistical analysis

Data were analyzed with the GraphPad Prism 7.0 software and presented as means ± SEM ($n \geq 3$). Two-sided *t* tests were used to determine the statistical difference between the means of two groups when sample sizes were small. Two-sided *P* values were also used in all analyses and $P < 0.05$ was considered to be statistically significant.

Extended Data

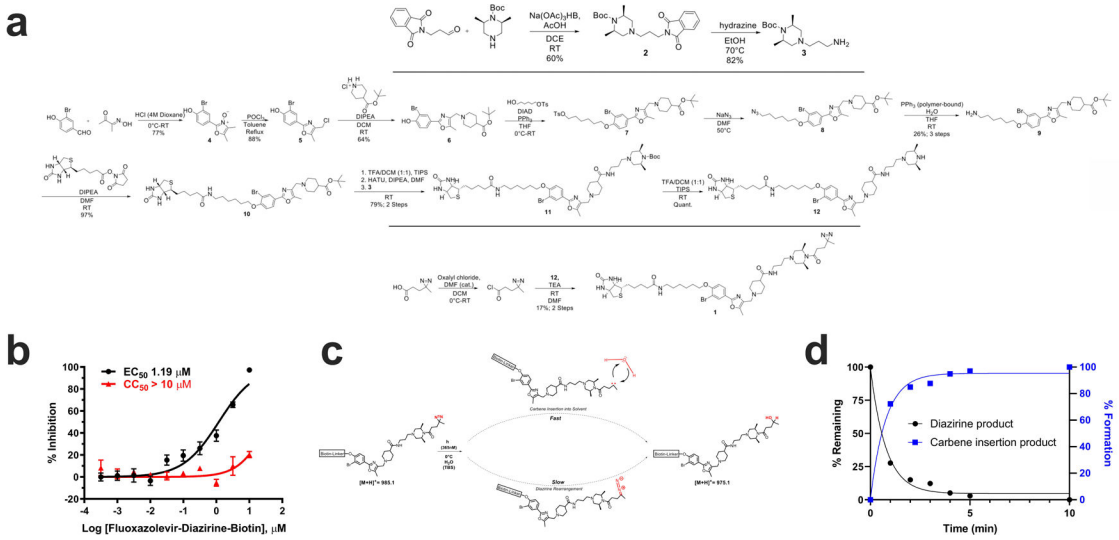

Extended Data Fig. 1. Synthesis, efficacy, and photolysis of the fluoxazolevir-diazirine-biotin probe.

a, The general synthetic scheme of the fluoxazolevir-diazirine-biotin (fluoxazolevir-DB) probe is shown. Each intermediate was confirmed with ^{1}H NMR and LCMS. See supplemental document for more information on each synthetic step. **b,** Fluoxazolevir-DB probe retains anti-HCV activity *in vitro* and shows inhibition against HCV infection in a dose-dependent manner. Data are presented as mean values ± SEM of 6 biologically independent replicates. **c,** The degradation of fluoxazolevir-DB via UV irradiation is shown. **d,** The fluoxazolevir-DB was exposed to UV irradiation with a 100 W mercury lamp with a 365 nm bypass filter. Disappearance of fluoxazolevir-DB was measured over time via LCMS and underwent a complete conversion to the carbene insertion product within 10 min. All results are representative of three independent experiments.

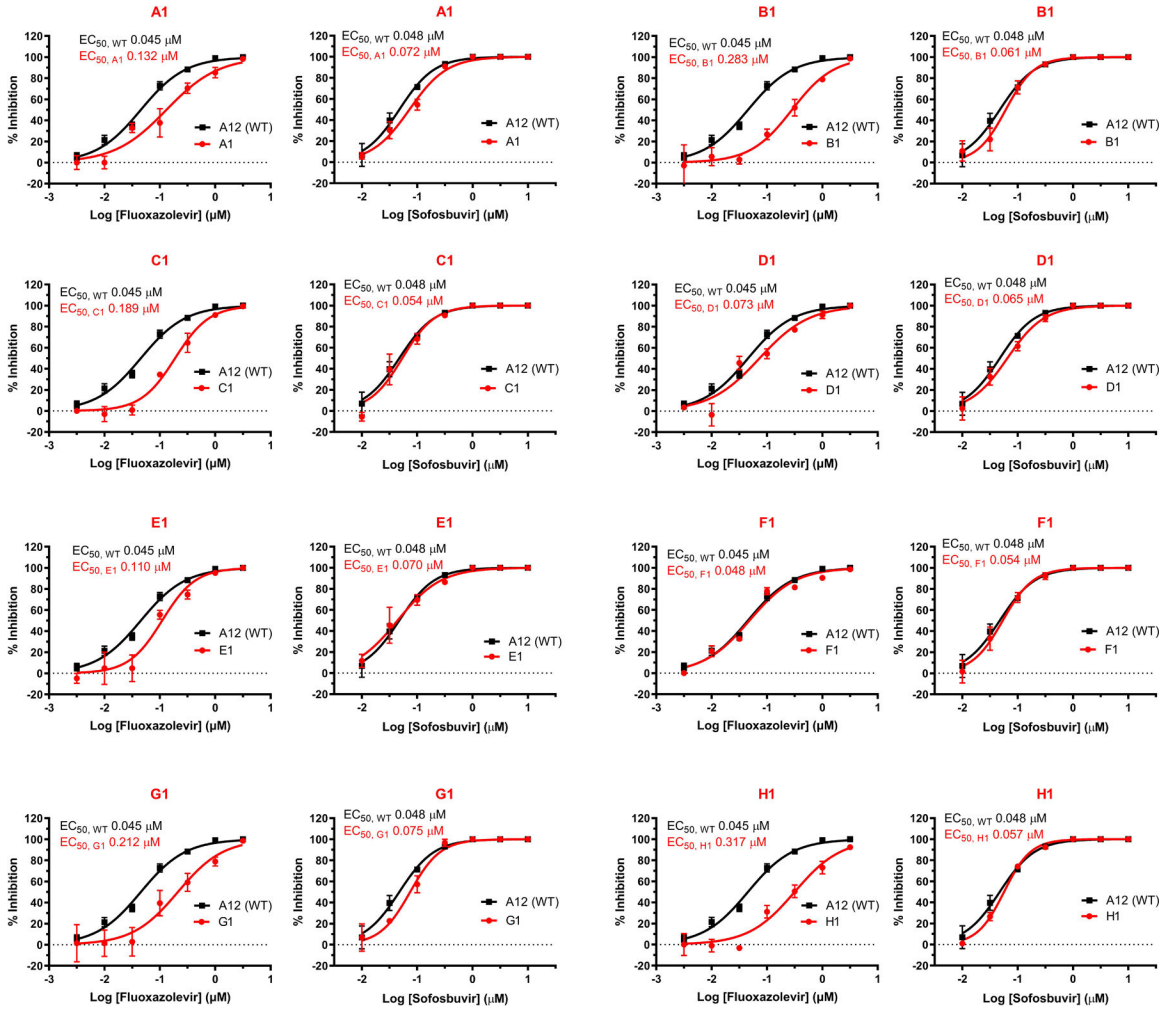

Extended Data Fig. 2. Dose-response curves of fluoxazolevir against amplified HCV from the *in vitro* drug resistance selection assay.

Among the 8 serial passages with potential RAS-containing HCV generated from the drug resistance selection assay (Fig. 2a), the viruses in the following wells (and their identified mutations) showed moderate resistance with EC_{50} values increasing by at least two-fold comparing to the wild-type control: A1 (F291L, V414A), B1 (I374T), C1 (D382E, T395A, M405V, P616A), E1 (F291V), G1 (A274S) and H1 (M267V, V284A). The same viruses were tested against sofosbuvir as a control and were equally sensitive to sofosbuvir as the wild type virus. Data are presented as mean values ± SEM of 3 biologically independent replicates. All results are representative of three independent experiments.

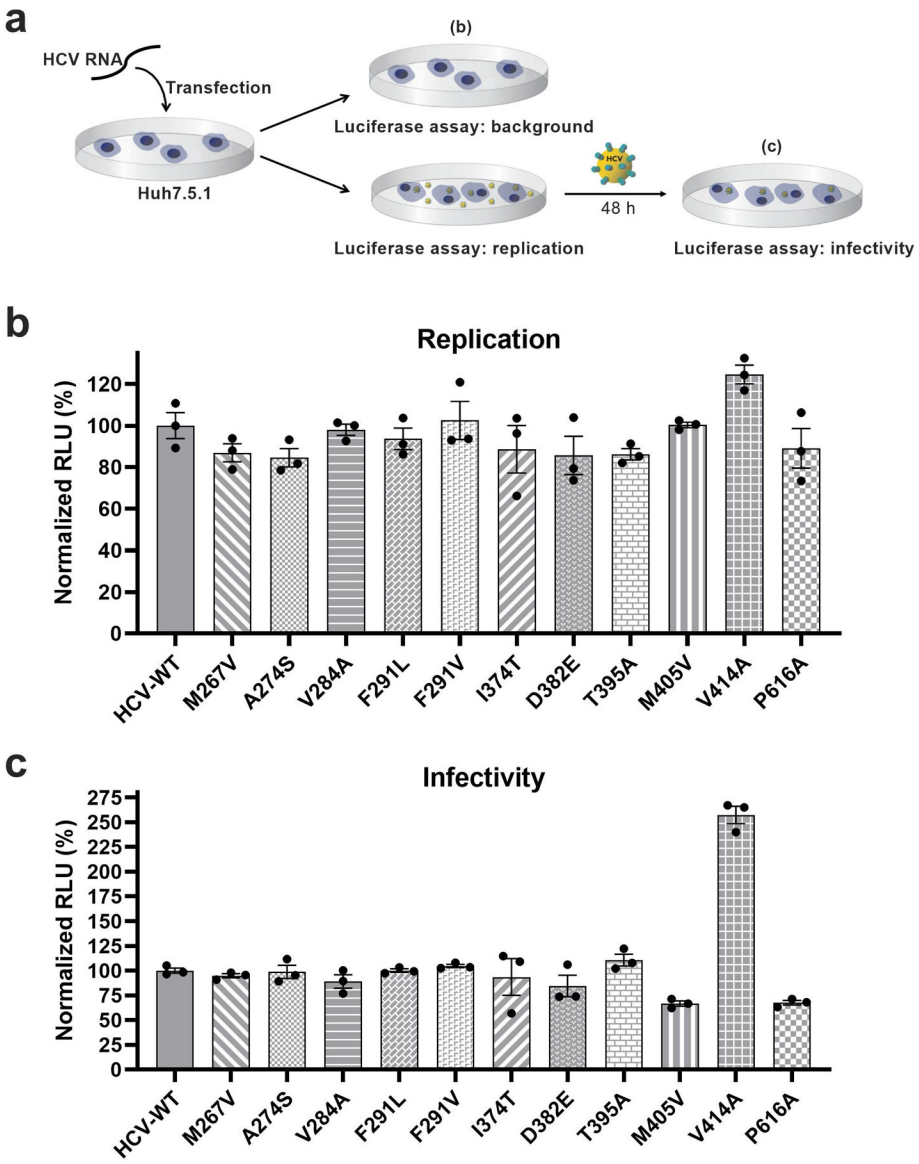

Extended Data Fig. 3. Viral fitness of the generated RAS-containing HCV.

a, The viral fitness assay scheme is shown here. Huh7.5.1 cells were electroporated with the RNA of each HCV RAS-RLuc construct. **b,** The first part of the assay assesses the replication capacity for each RAS-containing HCV. Luminescence was measured 4 h and 3 days after electroporation and the readings obtained 4 h after electroporation was used as background. **c**, The second part of the assay assesses infectivity of each RAS. Viral medium harvested 3 days after electroporation from part b was used to reinfect 10^4 naïve Huh7.5.1 cells in a 96-well plate. Luminescence was measured 48 h after reinfection and all measurements were normalized to HCV-WT. Data are presented as mean values ± SEM of 3 biologically independent replicates. All results are representative of three independent experiments.

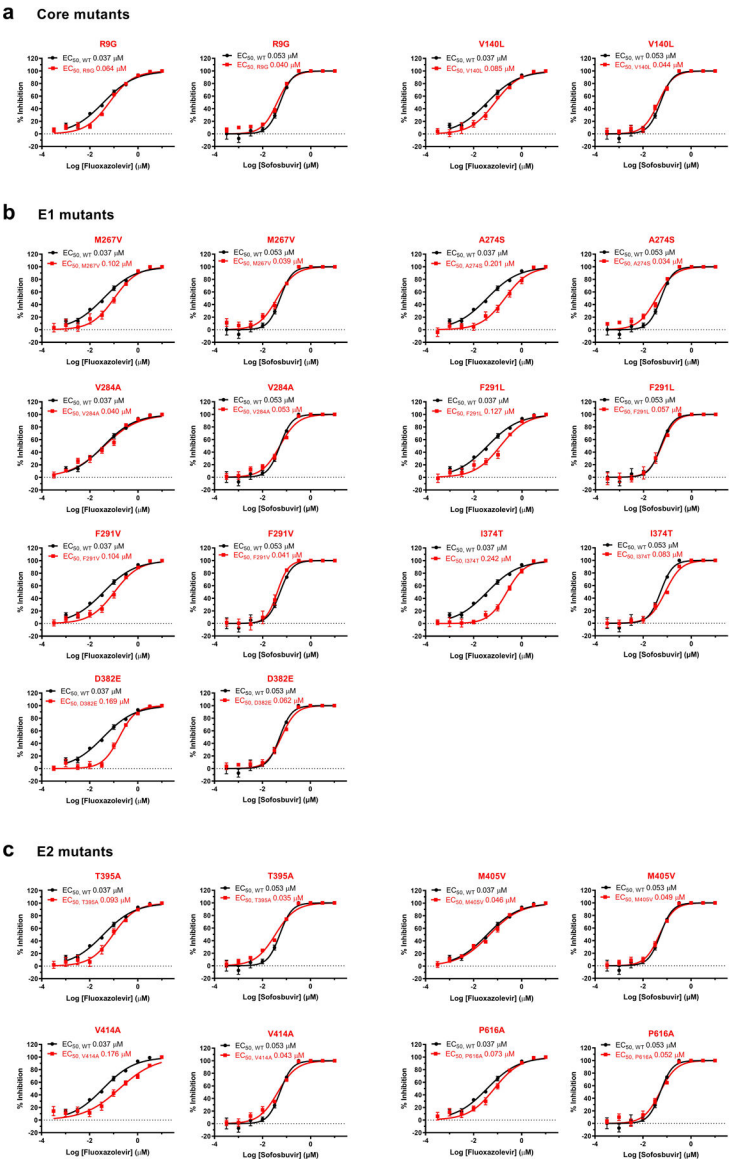

Extended Data Fig. 4. Dose-response curves of fluoxazolevir against HCV mutants with putative RASs in core, E1 and E2 regions.

Huh7.5.1 cells in 96-well plates were infected with wild-type HCV-RLuc (GT 2a) and HCV-RLuc mutants with various putative RASs (R9G, V140L, M267V, A274S, V284A, F291L, F291V, I374T, D382E, T395A, M405V, V414A and P616A) in the presence of various fluoxazolevir concentrations as indicated. Cells were harvested 48 h after infection and luminescence assessed via the luciferase assay. The EC_{50} values for wild-type HCV-RLuc (black circles) and the HCV mutants (red squares) were calculated with Prism 7. Data are presented as mean values ± SEM of 8 biologically independent replicates. All results are representative of three independent experiments.

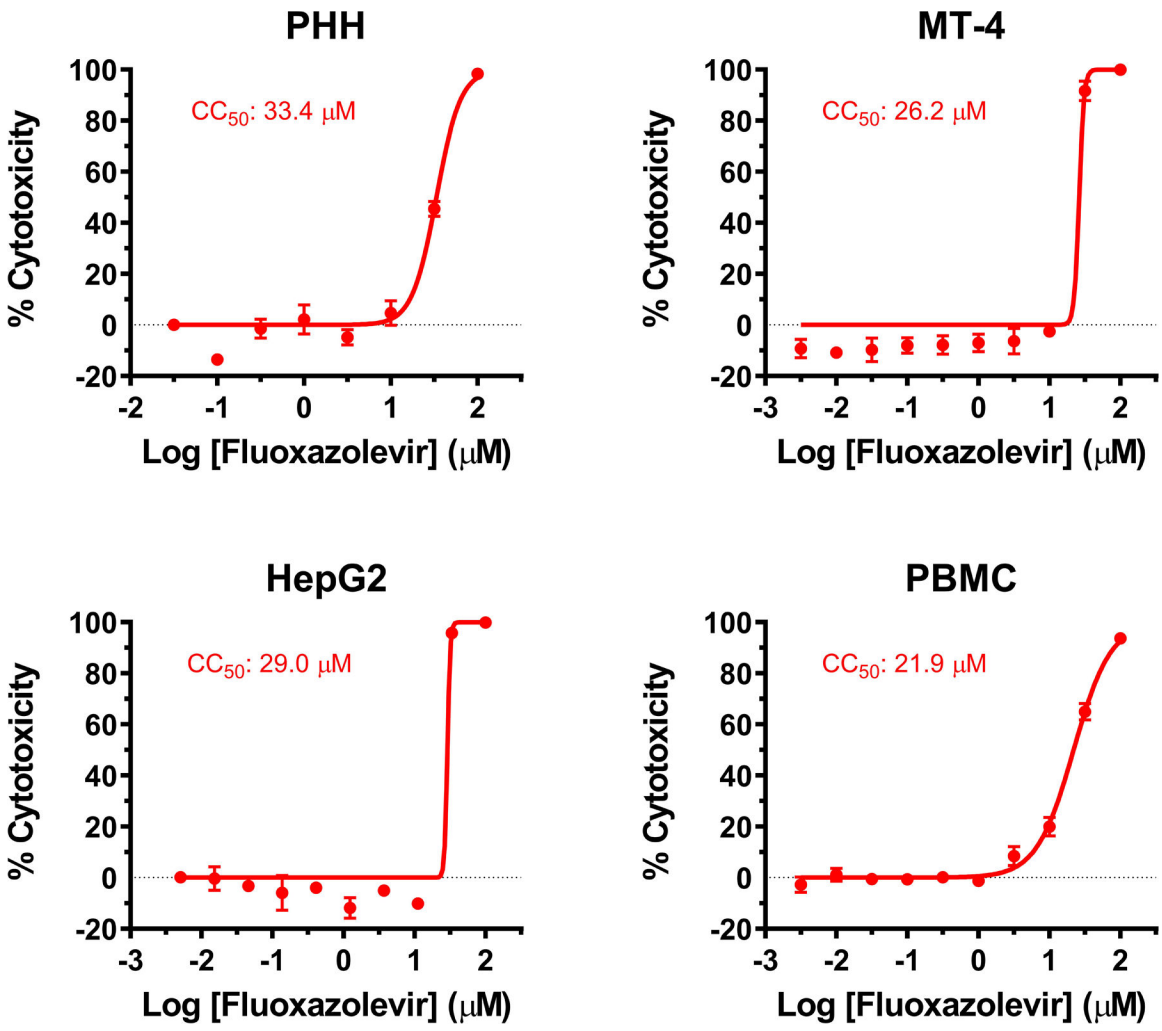

Extended Data Fig. 5. Cytotoxicity of fluoxazolevir against primary human hepatocytes, HepG2 cells, MT-4 cells and peripheral blood mononuclear cells.

Cells were treated with fluoxazolevir for 3 days and processed for the ATPlite cytotoxicity assay. CC_{50} values were calculated with the software, Prism 7. Data are presented as mean values ± SEM of 3 biologically independent replicates. All results are representative of three independent experiments.

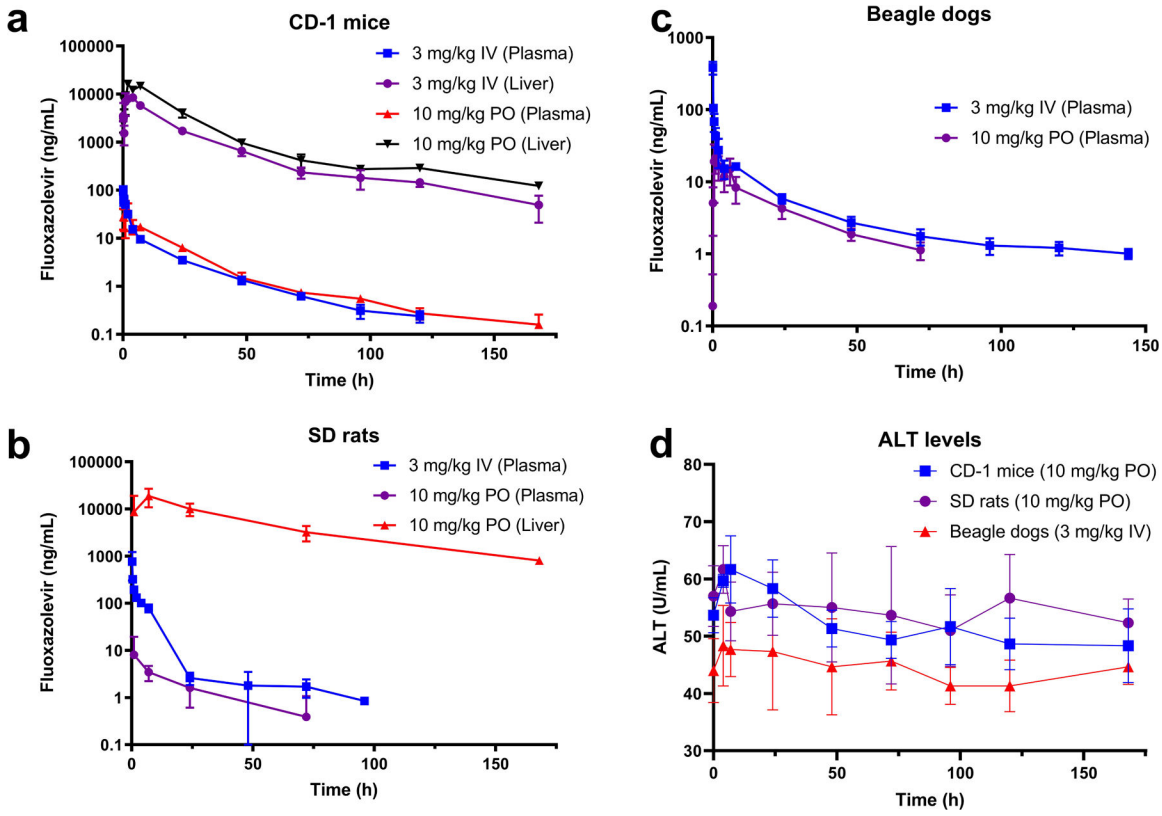

Extended Data Fig. 6. Pharmacokinetics of fluoxazolevir.

Pharmacokinetic studies of fluoxazolevir were performed in (**a**) male CD-1 mouse, (**b**) male SD rat and (**c**) male beagle dog models (n = 3 animals). The concentration profiles of fluoxazolevir were measured after either a single PO dose of 10 mg/kg or a single IV dose of 3 mg/kg. Compound concentrations were measured by UPLC-MS/MS. **d,** Serum alanine aminotransferase (ALT) levels were measured in each animal model to assess the potential toxicity of fluoxazolevir *in vivo*. For CD-1 mice and SD rats, ALTs from the 10 mg/kg PO groups were shown, and for beagle dogs, the 3 mg/kg IV group was shown. Data are presented as mean values ± standard deviations.

Animal	CD-1 Mouse[1] (n = 39)						SD Rat[1] (n = 12)	
Dose	PO (10 mg/kg)		PO (5 mg/kg)				PO (10 mg/kg)	
Sample	plasma	liver	plasma	liver	brain	heart	Plasma	Liver
$AUC_{0-\infty}$[2] (μM•h)	1.15	754	0.419	389	3.23	39.7	0.300	1870
$t_{1/2}$[2] (h)	37	45	27	26	58	32	21	37
T_{max}[2] (h)	2	2	1	7	7	24	1	7
C_{max}[2] (μM)	0.084	34.4	0.031	13.8	0.042	0.78	0.017	39.9
AUC ratio (Tissue/Plasma)	-	659	-	929	7.7	95	-	6250

Extended Data Fig. 7. Tissue distribution of fluoxazolevir after PO administration in rodents.

[1] The plasma and tissue concentrations of fluoxazolevir were measured after a single PO dose of fluoxazolevir. [2] $AUC_{0-\infty}$: area under the curve from zero to infinity; $t_{1/2}$: half-life;

T_{max}: time to reach the maximal concentration; C_{max}: maximal concentration after PO administration.

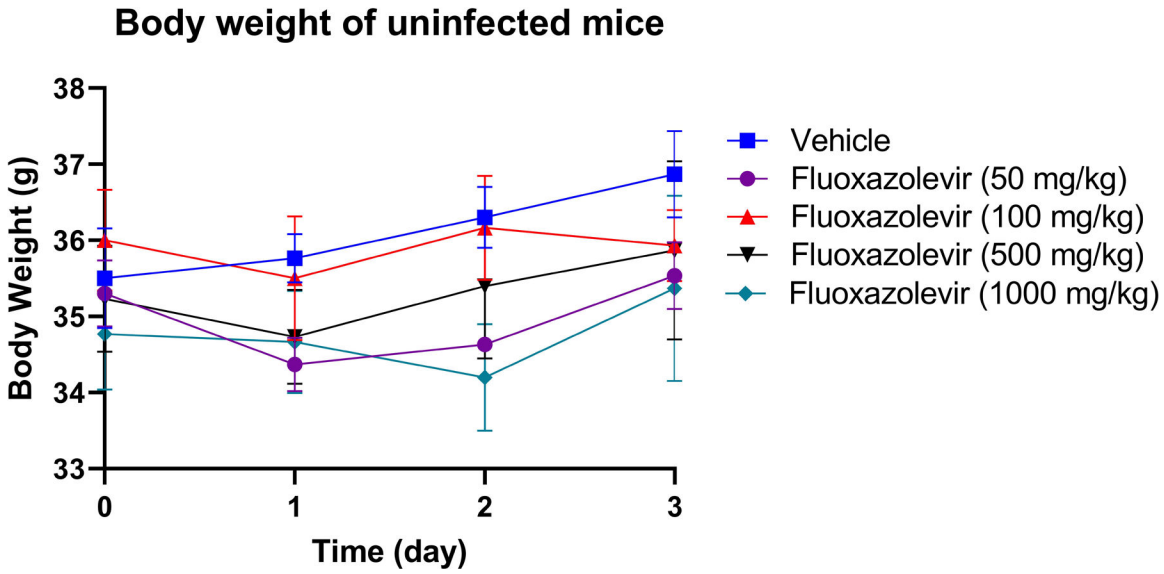

Extended Data Fig. 8. Maximal tolerable dose of fluoxazolevir in mice.

The study was performed by Pharmaron Inc. (Beijing, PR China). Single doses of fluoxazolevir (50 mg/kg, 100 mg/kg, 500 mg/kg and 1000 mg/kg) were administered via oral gavage to CD-1 mice (n=3 mice per group) and observed for 3 days. Body weights of all animals were recorded daily. All study animals were monitored behavior such as respite, food and water consumption (by cage side checking), circling, eye/hair matting and any other abnormal effect. Any mortality and/or abnormal clinical signs were recorded. All animals were sacrificed for necropsy on day 3. Data are presented as mean values ± SEM.

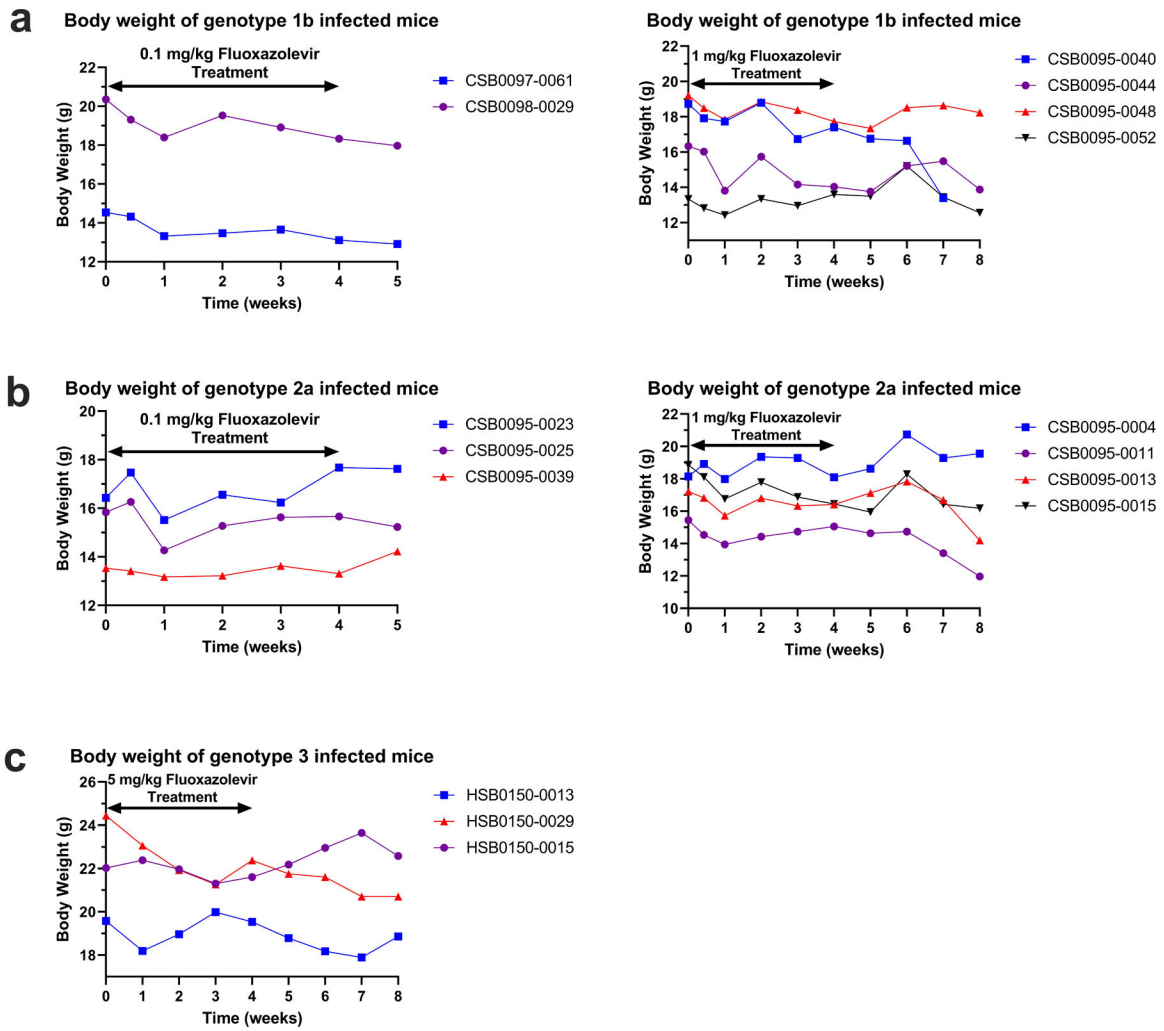

Extended Data Fig. 9. Lack of toxicity of fluoxazolevir monotherapy in genotypes 1b, 2a and 3-infected *Alb-uPA/Scid* mice.

The body weights of the humanized *Alb-uPA/Scid* mice infected with HCV genotypes **(a)** 1b (n=2–4 mice), **(b)** 2a (n=3–4 mice) and **(c)** 3 (n=3 mice) were monitored during and after fluoxazolevir treatment as described in Fig. 4a & b, Supp. Fig. 3–5. All mice in each group were weighed regularly for evidence of toxicity.

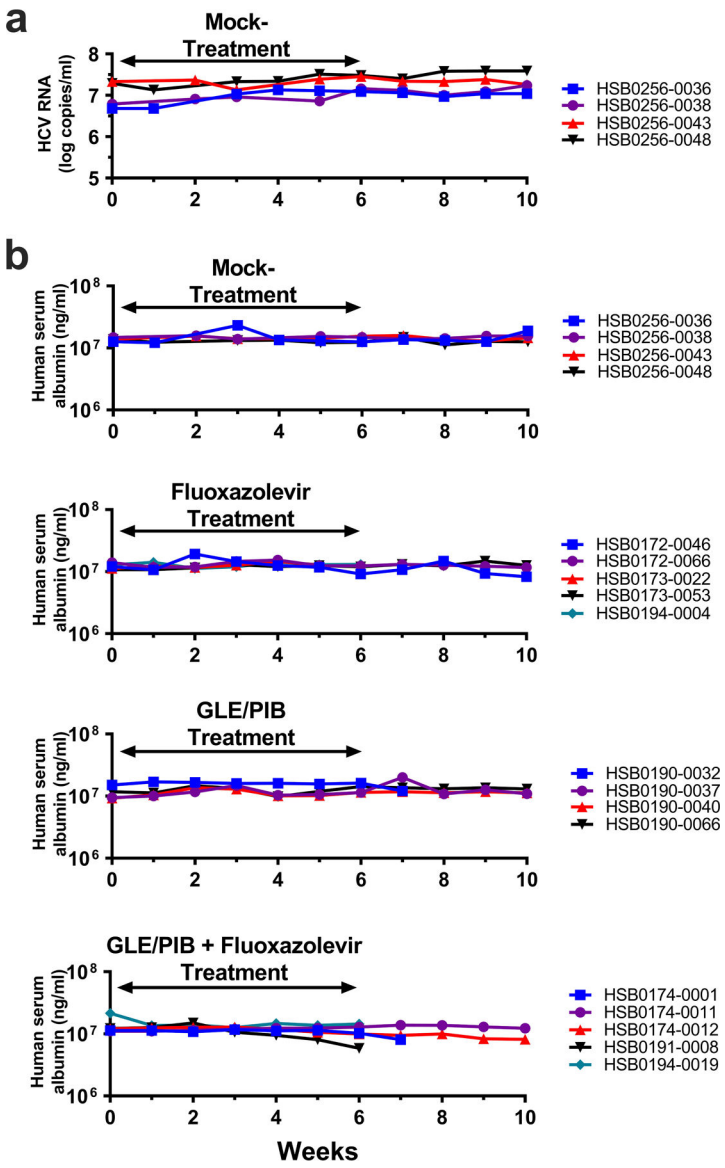

Extended Data Fig. 10. HCV RNA and serum human albumin levels of mice infected with multidrug-resistant HCV.

Humanized *Alb-uPA/Scid* mice were infected with the multidrug-resistant HCV strain and were either untreated (n = 4 mice) or treated with fluoxazolevir (n = 5 mice), GLE/PIB (n = 4 mice) or combination (n = 5 mice). Serum HCV RNA and human serum albumin levels were monitored weekly. **a,** Serum HCV RNA levels of untreated humanized *Alb-uPA/Scid* mice showed steady levels during follow-up. Time 0 is comparable to the time of initiation of treatment in (b). Mouse serum samples at the end of the 20 weeks were sequenced and the same NS3 and NS5a mutations as the inoculum virus were identified. **b,** Mice treated with fluoxazolevir (5 mg/kg), glecaprevir (60 mg/kg) and pibrentasvir (24 mg/kg). Weekly serum levels of HCV RNA and human albumin of each individual mouse were plotted. Weekly HCV RNA measurements of individual mice for each time point are shown in Fig. 4c. Serum human albumin graphs that end before the 10 weeks are due to death of the mice.

Supplementary Material

Refer to Web version on PubMed Central for supplementary material.

Acknowledgment

This work was supported by the Intramural Research Program of the National Institute of Diabetes and Digestive and Kidney Diseases and National Center for Advancing Translational Sciences, National Institutes of Health, USA, the Molecular Libraries Initiative funding to the University of Kansas Specialized Chemistry Center (U54HG005031) and the Japan Agency for Medical Research and Development (JP18fk0210020h0002).

References

1. Blach S, et al. Global prevalence and genotype distribution of hepatitis C virus infection in 2015: a modelling study. Lancet Gastroenterol Hepatol 2, 161–176 (2017). [PubMed: 28404132]
2. Jafari S, Copes R, Baharlou S, Etminan M & Buxton J Tattooing and the risk of transmission of hepatitis C: a systematic review and meta-analysis. Int. J. Infect. Dis 14, e928–e940 (2010). [PubMed: 20678951]
3. Blackard JT, Shata MT, Shire NJ & Sherman KE Acute hepatitis C virus infection: A chronic problem. Hepatology 47, 321–331 (2008). [PubMed: 18161707]
4. Liang TJ & Ghany MG Current and future therapies for hepatitis C virus infection. N. Engl. J. Med 368, 1907–1917 (2013). [PubMed: 23675659]
5. Liang TJ & Ghany MG Therapy of hepatitis C--back to the future. N. Engl. J. Med 370, 2043–2047 (2014). [PubMed: 24795199]
6. Ward JW & Hinman AR What is needed to eliminate hepatitis B virus and hepatitis C virus as global health threats. Gastroenterology 156, 297–310 (2019). [PubMed: 30391470]
7. Zeuzem S et al. Sofosbuvir and ribavirin in HCV genotypes 2 and 3. N. Engl. J. Med 370, 1993–2001 (2014). [PubMed: 24795201]
8. Fourati S, et al. Frequent antiviral treatment failures in patients infected with hepatitis C virus genotype 4, subtype 4r. Hepatology 69, 513–523 (2019). [PubMed: 30125371]
9. Childs K, et al. Suboptimal SVR rates in African patients with atypical genotype 1 subtypes: Implications for global elimination of hepatitis C. J. Hepatol 71, 1099–1105 (2019). [PubMed: 31400349]
10. Wei L, et al. Sofosbuvir-velpatasvir for treatment of chronic hepatitis C virus infection in Asia: a single-arm, open-label, phase 3 trial. Lancet Gastroenterol. Hepatol 4, 127–134 (2019). [PubMed: 30555048]
11. Garrison KL, German P, Mogalian E & Mathias A The drug-drug interaction potential of antiviral agents for the treatment of chronic hepatitis C infection. Drug Metab. Dispos 46, 1212–1225 (2018). [PubMed: 29695614]
12. Voelker R The 8-week cure for hepatitis C. JAMA 318, 996–996 (2017).
13. Pawlotsky JM Hepatitis C virus resistance to direct-acting antiviral drugs in interferon-free regimens. Gastroenterology 151, 70–86 (2016). [PubMed: 27080301]
14. Oral Abstracts (Abstract 200, 204) Hepatology 68, 1–183 (2018).
15. Di Maio VC, et al. Frequent NS5A and multiclass resistance in almost all HCV genotypes at DAA failures: What are the chances for second-line regimens? J. Hepatol 68, 597–600 (2018). [PubMed: 28939133]
16. Teegen EM, Maurer MM, Globke B, Pratschke J & Eurich D Liver transplantation for Hepatitis-B-associated liver disease - Three decades of experience. Transpl. Infect. Dis 21, e12997 (2019). [PubMed: 30203903]
17. Hu Z, et al. Novel cell-based hepatitis C virus infection assay for quantitative high-throughput screening of anti-hepatitis C virus compounds. Antimicrob. Agents Chemother 58, 995–1004 (2014). [PubMed: 24277038]
18. He S et al. Development of an aryloxazole class of hepatitis C virus inhibitors targeting the entry stage of the viral replication cycle. J. Med. Chem 60, 6364–6383 (2017). [PubMed: 28636348]

19. He S et al. Repurposing of the antihistamine chlorcyclizine and related compounds for treatment of hepatitis C virus infection. Sci. Transl. Med 7, 282ra249 (2015).
20. Tscherne DM, et al. Time- and temperature-dependent activation of hepatitis C virus for low-pH-triggered entry. J. Virol 80, 1734–1741 (2006). [PubMed: 16439530]
21. Ashfaq UA, Javed T, Rehman S, Nawaz Z & Riazuddin S Lysosomotropic agents as HCV entry inhibitors. Virol J 8, 163–163 (2011). [PubMed: 21481279]
22. Sharma NR, et al. Hepatitis C virus is primed by CD81 protein for low pH-dependent fusion. J. Biol. Chem 286, 30361–30376 (2011). [PubMed: 21737455]
23. Bush CO, et al. A small-molecule inhibitor of hepatitis C virus infectivity. Antimicrob. Agents Chemother 58, 386–396 (2014). [PubMed: 24165192]
24. Zhou N, et al. Characterization of NS5A polymorphisms and their impact on response rates in patients with HCV genotype 2 treated with daclatasvir-based regimens. J. Antimicrob. Chemother 71, 3495–3505 (2016). [PubMed: 27605597]
25. Gottwein JM, et al. Development and characterization of hepatitis C virus genotype 1–7 cell culture systems: Role of CD81 and scavenger receptor class B type I and effect of antiviral drugs. Hepatology 49, 364–377 (2009). [PubMed: 19148942]
26. Lin B, He S, Yim HJ, Liang TJ & Hu Z Evaluation of antiviral drug synergy in an infectious HCV system. Antivir. Ther 21, 595–603 (2016). [PubMed: 27035622]
27. Bijnsdorp IV, Giovannetti E & Peters GJ Analysis of drug interactions in Cancer Cell Culture: Methods and Protocols (ed. Cree IA) 421–434 (Humana Press, Totowa, NJ, 2011).
28. Prichard MN & Shipman C A three-dimensional model to analyze drug-drug interactions. Antiviral Res 14, 181–205 (1990). [PubMed: 2088205]
29. Puoti M, et al. High SVR12 with 8-week and 12-week glecaprevir/pibrentasvir therapy: An integrated analysis of HCV genotype 1–6 patients without cirrhosis. J. Hepatol 69, 293–300 (2018). [PubMed: 29551706]
30. Ng TI, et al. In vitro antiviral activity and resistance profile of the next-generation hepatitis C virus NS3/4A protease inhibitor glecaprevir. Antimicrob. Agents Chemother 62, e01620–01617 (2017). [PubMed: 29084747]
31. Ng TI, et al. In vitro antiviral activity and resistance profile of the next-generation hepatitis C virus NS5A inhibitor pibrentasvir. Antimicrob. Agents Chemother 61, e02558–02516 (2017). [PubMed: 28193664]
32. Osawa M, et al. Real-world efficacy of glecaprevir plus pibrentasvir for chronic hepatitis C patient with previous direct-acting antiviral therapy failures. J. Gastroenterol 54, 291–296 (2019). [PubMed: 30334096]
33. Osawa M, et al. Efficacy of glecaprevir and pibrentasvir treatment for genotype 1b hepatitis C virus drug resistance-associated variants in humanized mice. J. Gen. Virol 100, 1123–1131 (2019). [PubMed: 31199224]
34. Krishnan P, et al. Pooled resistance analysis in patients with hepatitis C virus genotype 1 to 6 infection treated with glecaprevir-pibrentasvir in phase 2 and 3 clinical trials. Antimicrob. Agents Chemother 62, e01249–01218 (2018). [PubMed: 30061289]
35. Li HF, Huang CH, Ai LS, Chuang CK & Chen SS Mutagenesis of the fusion peptide-like domain of hepatitis C virus E1 glycoprotein: involvement in cell fusion and virus entry. J. Biomed. Sci 16, 89 (2009). [PubMed: 19778418]
36. Tong Y, Lavillette D, Li Q & Zhong J Role of hepatitis C virus envelope glycoprotein E1 in virus entry and assembly. Front. Immunol 9, 1411–1411 (2018). [PubMed: 29971069]
37. Hu Z, et al. Chlorcyclizine inhibits viral fusion of hepatitis C virus entry by directly targeting HCV envelope glycoprotein 1. Cell Chem. Biol S2451–9456(20)30143–4 (2020).
38. Cocquerel L, Wychowski C, Minner F, Penin F & Dubuisson J Charged residues in the transmembrane domains of hepatitis C virus glycoproteins play a major role in the processing, subcellular localization, and assembly of these envelope proteins. J. Virol 74, 3623–3633 (2000). [PubMed: 10729138]
39. Freedman H, et al. Computational prediction of the heterodimeric and higher-order structure of gpE1/gpE2 envelope glycoproteins encoded by hepatitis C virus. J. Virol 91, e02309–02316 (2017). [PubMed: 28148799]

40. Partridge AW, Therien AG & Deber CM Missense mutations in transmembrane domains of proteins: Phenotypic propensity of polar residues for human disease 54, 648–656 (2004).
41. Kong L, et al. Hepatitis C virus E2 envelope glycoprotein core structure. Science 342, 1090–1094 (2013). [PubMed: 24288331]
42. Serre SBN, Krarup HB, Bukh J & Gottwein JM Identification of alpha interferon-induced envelope mutations of hepatitis C virus in vitro associated with increased viral fitness and interferon resistance. J. Virol 87, 12776–12793 (2013). [PubMed: 24049176]
43. Bogomolov P, et al. Treatment of chronic hepatitis D with the entry inhibitor myrcludex B: First results of a phase Ib/IIa study. J. Hepatol 65, 490–498 (2016). [PubMed: 27132170]
44. Bethea ED, et al. Pre-emptive pangenotypic direct acting antiviral therapy in donor HCV-positive to recipient HCV-negative heart transplantation: an open-label study. Lancet Gastroenterol. Hepatol 4, 771–780 (2019). [PubMed: 31353243]
45. Woolley AE, et al. Heart and lung transplants from HCV-infected donors to uninfected recipients. N. Engl. J. Med 380, 1606–1617 (2019). [PubMed: 30946553]
46. Rolt A, et al. Preclinical pharmacological development of chlorcyclizine derivatives for the treatment of hepatitis C virus infection. J. Infect. Dis 217, 1761–1769 (2018). [PubMed: 29373739]
47. Perin PM, et al. Flunarizine prevents hepatitis C virus membrane fusion in a genotype-dependent manner by targeting the potential fusion peptide within E1. Hepatology 63, 49–62 (2016). [PubMed: 26248546]
48. Vausselin T, et al. Identification of a new benzimidazole derivative as an antiviral against hepatitis C virus. J. Virol 90, 8422–8434 (2016). [PubMed: 27412600]
49. Harrison SC Viral membrane fusion. Virology 498–507 (2015). [PubMed: 25866377]
50. Rybak J-N, Scheurer SB, Neri D & Elia G Purification of biotinylated proteins on streptavidin resin: A protocol for quantitative elution. Proteomics 4, 2296–2299 (2004). [PubMed: 15274123]

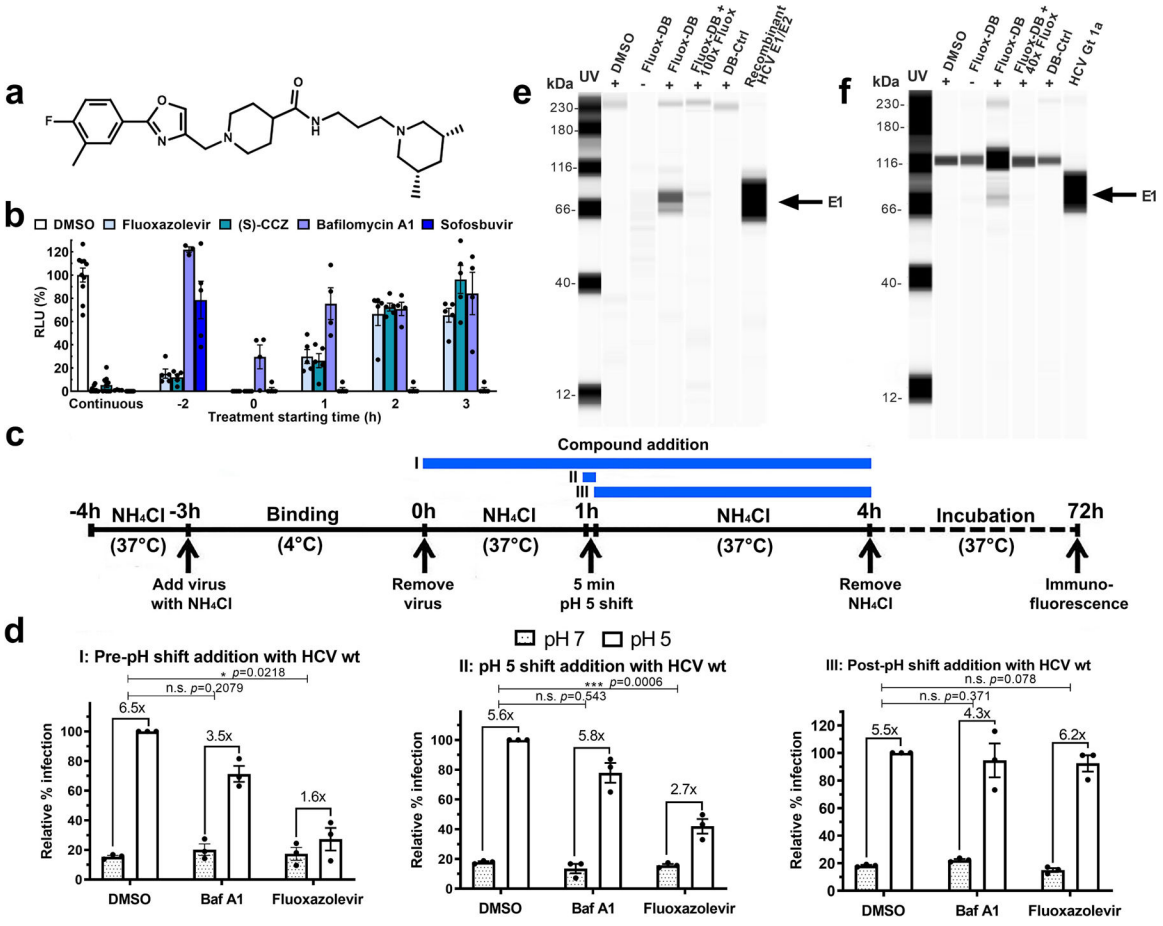

Fig. 1. Fluoxazolevir disrupts HCV membrane fusion.

a, The structure of fluoxazolevir is shown. **b,** The time-of-addition assay was performed with fluoxazolevir and other controls (See Methods). Results were normalized to the DMSO continuous treatment. Data are presented as mean values ± SEM (n=4–10 biological independent samples). **c,** The membrane fusion assay scheme shows three protocols where the compound (fluoxazolevir, bafilomycin A1 or DMSO) was added at various time points (See Methods). **d,** Huh7.5.1 cells were stained by HCV core immunofluorescence. The numbers of HCV positive foci (≥ 5 stained cells in each group) were counted in each well. Data were normalized to the DMSO continuous treatment and presented as mean values ± SEM (n=3 biological independent samples). Statistical significance of the fold-changes between the pH 7 and pH 5 shift was compared to the DMSO control within each protocol (two-sided Student's *t* test). **e,** Fluoxazolevir-DB was used in a cross-linking experiment with genotype 1a recombinant HCV E1/E2 protein (See Methods in Supp. Information). Recombinant E1/E2 protein was included on the blot as a reference. **f,** After the addition of fluoxazolevir-DB to HCV genotype 1a-infected Huh7.5.1 cells, the cells were subjected to UV cross-linking and lysis (See Methods). High-titer HCV genotype 1a virus generated in cell culture was included on the blot as a reference. In one sample, an excess amount of fluoxazolevir (200 μM) was added with fluoxazolevir-DB (2 μM for *in vitro* and 5 μM for infected cells) prior to the cross-linking reaction. The results are representative of three independent experiments.

a

Well Location (passage #)	Region	Mutations
A1 (p27)	Core	V140L
	E1	F291L
	E2	V414A
B1 (p27)	Core	R9G
	E1	I374T
	E2	None
C1 (p27)	Core	None
	E1	D382E
	E2	T395A, M405V, P616A
D1 (p27)	Core	None
	E1	None
	E2	None
E1 (p27)	Core	None
	E1	F291V
	E2	None
F1 (p27)	Core	None
	E1	None
	E2	None
G1 (p27)	Core	None
	E1	A274S
	E2	None
H1 (p27)	Core	None
	E1	M267V, V284A
	E2	None

c

HCV	Fluoxazolevir		Sofosbuvir	
	EC_{50} (μM)	Max Resp. ± SEM (%) at 1 μM	EC_{50} (μM)	Max Resp. ± SEM (%) at 10 μM
WT	0.037	93.3 ± 1.1	0.053	100 ± 0
R9G	0.064	92.9 ± 1.0	0.040	100 ± 0
V140L	0.078	93.3 ± 1.1	0.044	100 ± 0
M267V	0.102	90.4 ± 1.5	0.056	100 ± 0
V284A	0.040	92.3 ± 0.8	0.055	100 ± 0
A274S	0.201	78.2 ± 5.2	0.045	100 ± 0
F291L	0.127	88.9 ± 1.8	0.054	100 ± 0
F291V	0.104	87.9 ± 1.8	0.045	100 ± 0
I374T	0.242	93.3 ± 1.1	0.080	100 ± 0
D382E	0.169	87.5 ± 0.8	0.062	100 ± 0
T395A	0.094	89.8 ± 1.4	0.035	100 ± 0
M405V	0.044	91.3 ± 1.6	0.049	100 ± 0
V414A	0.176	69.3 ± 3.3	0.046	100 ± 0
P616A	0.073	91.1 ± 1.7	0.052	100 ± 0

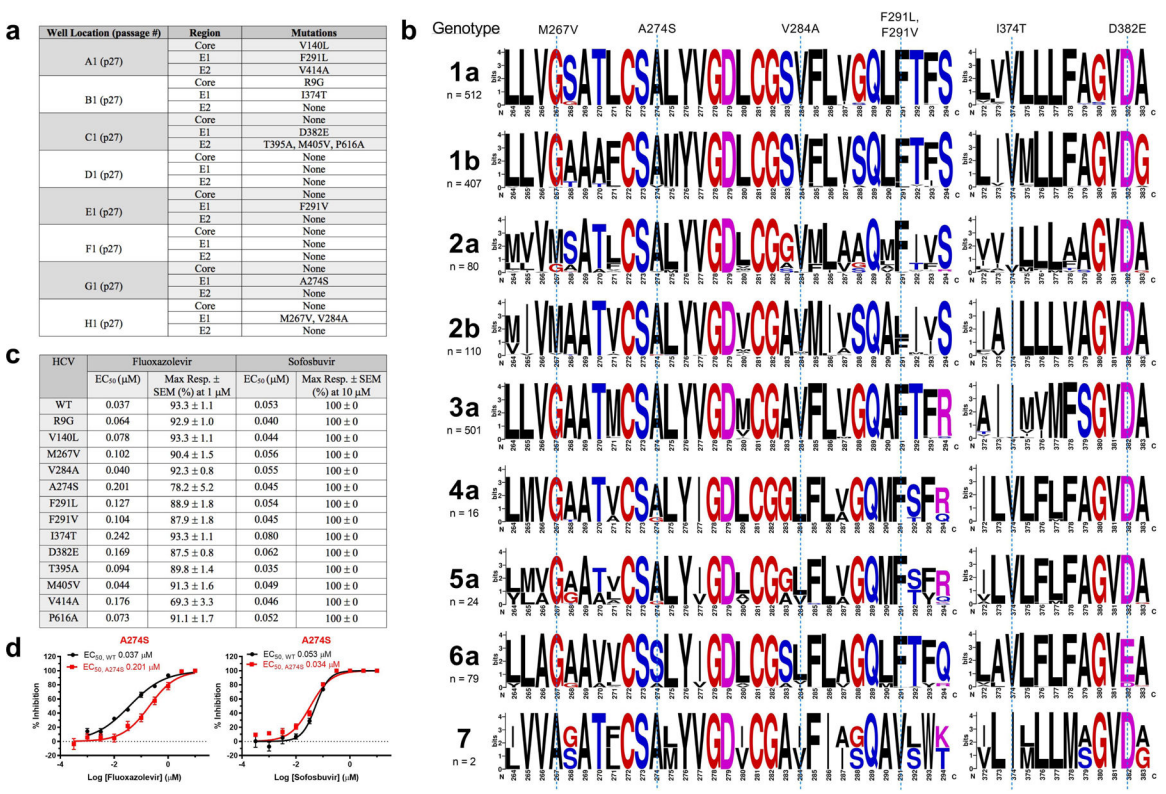

Fig. 2. Fluoxazolevir-resistant HCV substitutions generated from the *in vitro* resistance selection assay.

a, A fluoxazolevir concentration gradient was established in a 96-well plate with HCV J6/JFH1 where the concentrations were 5 μM in column 1 and 0 μM in column 12. Mutations that emerged in the vehicle-only control (Supp. Fig. 1, column 12, DMSO) were not included because they most likely represented naturally evolved mutations with each passage. The detected mutations were I313V, N417S, I438V, L524F, I678V and L744S. **b**, Partial E1 sequences of all major genotypes, except for genotype 7, were obtained from the Virus Pathogen Resource database and were aligned between residues 264 and 294, and between residues 372 and 383. Genotype 7 sequences were obtained from NCBI. The n of each genotype sequence in the analysis is shown. Putative E1 RASs against fluoxazolevir are indicated. MAFFT version 7 with the G-INS-1 progressive method and Berkeley WebLogo were used to generate the alignment figure. **c**, The EC_{50} values and maximal percent inhibition responses are summarized here for all the generated RASs against fluoxazolevir or sofosbuvir and further detailed in Extended Data Fig. 4. Fluoxazolevir inhibits HCV J6/JFH1 infection close to 100% at concentrations above 1 μM for all RASs so the maximal response for each virus strain was reported at 1 μM. **d**, Representative dose-response curves of one RAS (A274S) against fluoxazolevir and sofosbuvir are shown here (n=6 biologically independent samples) and the rest in Extended Data Fig. 4. Data are presented as mean values ± SEM.

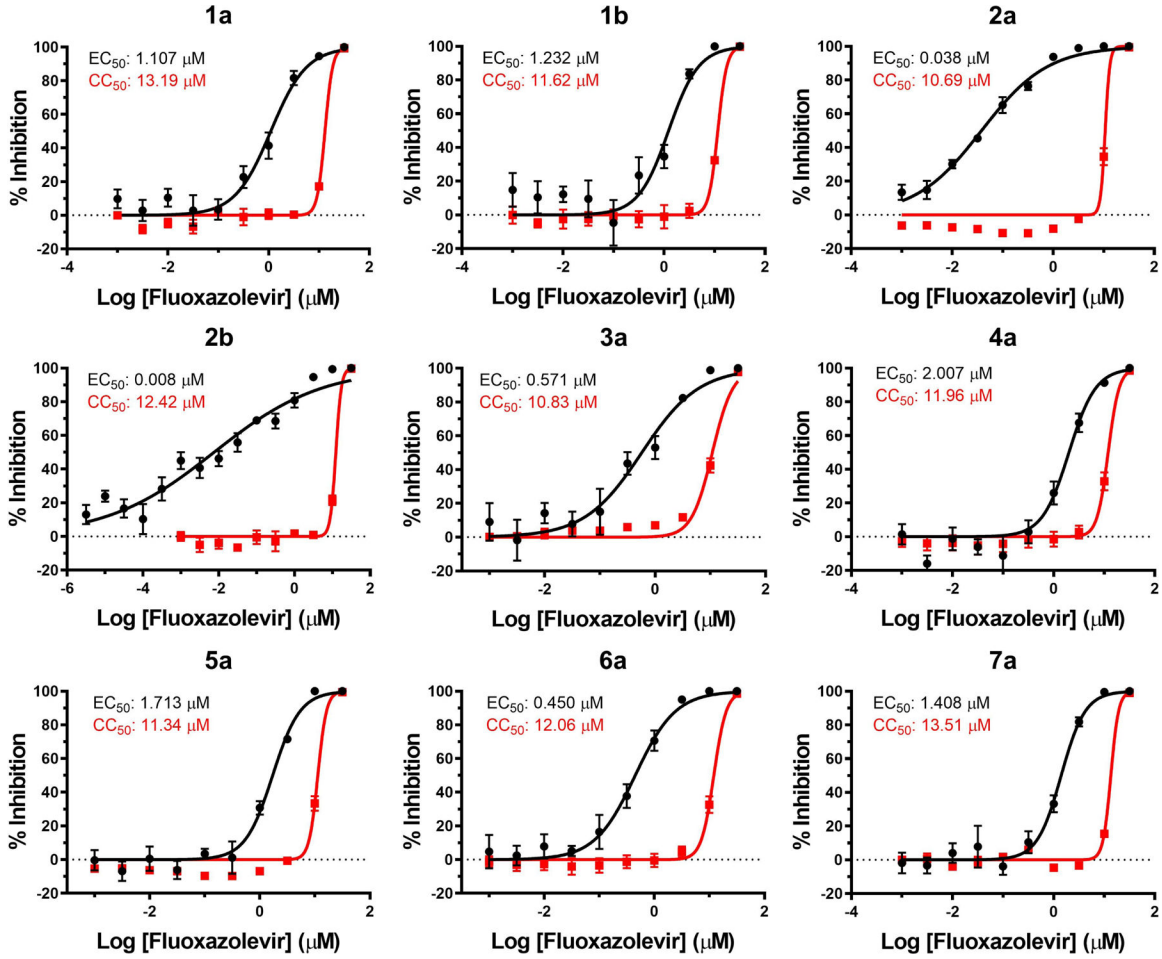

Fig. 3. Dose-response curves of fluoxazolevir against various chimeric HCV genotypes.

Huh7.5.1 cells in 96-well plates were infected with various chimeric HCV-RLuc (1a, 1b, 2b, 3a, 4a, 5a, 6a and 7a) together with fluoxazolevir at concentrations as indicated. Cells were harvested 48 h after infection to assess luminescence via the luciferase assay (black triangles). A parallel plate with the same treatment was processed for the ATPlite cytotoxicity assay (red squares). EC_{50} and CC_{50} values are calculated with the software, Prism 7. Dose-response curves of HCV-RLuc (GT 2a) are used as a reference. Each data point was presented as mean value ± SEM of 6 biological independent replicates and the results are representative of three independent experiments.

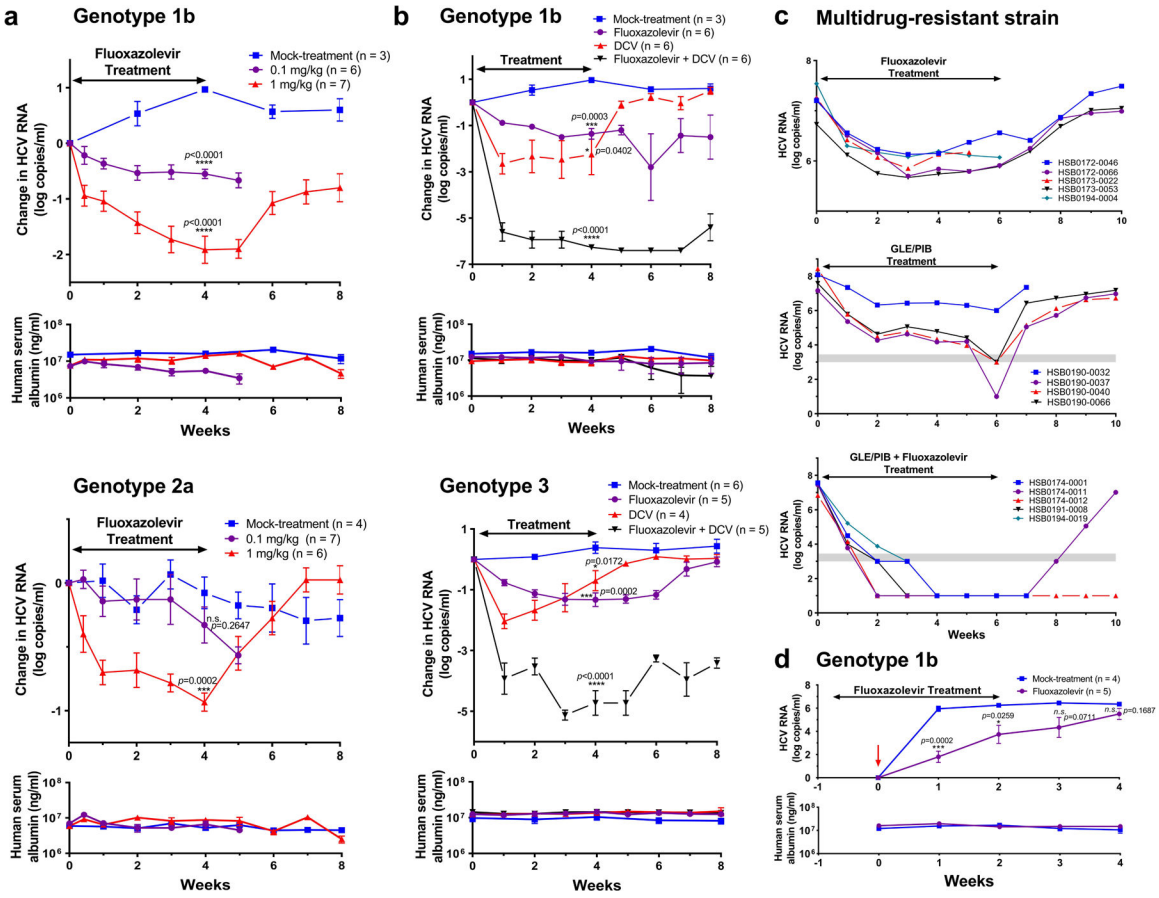

Fig. 4. Efficacy of fluoxazolevir *in vivo* against HCV genotypes 1b, 2a and 3 and multidrug-resistant HCV infection in *Alb-uPA/Scid* mice.

a, *Alb-uPA/Scid* mice infected with HCV genotype 1b or 2a were mock-treated or treated with 0.1 or 1 mg/kg fluoxazolevir. **b**, Mice infected with genotype 1b or 3 were untreated or treated with 5 mg/kg fluoxazolevir, 10 mg/kg daclatasvir or both daily for 4 weeks. For the combination-treated mice, all samples from week 1 had serum HCV RNA levels below the quantification limit of 3.45 $\log_{10}$ copies/ml. Changes in HCV RNA levels from the baseline are determined for each treated mouse and each data point is shown as mean value ± SEM. Statistical significance of change in HCV viremia at the end of treatment was compared to the mock-treatment control within each protocol (two-sided Student's *t* test). Individual mouse data for (**a)** & (**b)** are shown in Supp. Figs. 3–5. **c**, Mice were infected with a multidrug-resistant HCV strain and treated with 5 mg/kg fluoxazolevir, glecaprevir (60 mg/kg)/pibrentasvir (24 mg/kg), or both daily for 6 weeks. HCV viremia of untreated infected mice and individual mouse serum albumin data are shown in Extended Data Fig. 10. Serum HCV RNA levels from individual mice are shown and graphs that end before 10 weeks are due to death of the mice. The gray area represents the lower limit of quantification (3.45 $\log_{10}$ copies/ml) and lower limit of detection (3 $\log_{10}$ copies/ml) for HCV RNA levels. **d**, A group of *Alb-uPA/Scid* mice were mock-treated or treated daily with 1 mg/kg fluoxazolevir five days before and two weeks after HCV infection. HCV RNA levels and human serum albumin were monitored weekly. Statistical significance of change in HCV viremia at each time point is shown (two-sided Student's *t* test). Individual mouse data are

shown in Supp. Fig. 6. The number of mice (n) for each experimental group of a, b and d is shown on the graph. Data are presented as mean values ± SEM.

Table 1.

Synergistic activity of fluoxazolevir with selected HCV drugs

Program	Parameter	Sofosbuvir	Ribavirin	Daclatasvir	Simeprevir	Interferon-α
CalcuSyn	CI value[1]	0.302 ± 0.019	0.375 ± 0.050	0.202 ± 0.078	0.421 ± 0.097	0.365 ± 0.051
	Synergy volume[2]	+++	+++	+++	+++	+++
MacSynergy II	Log volume[3]	73.07	5.97	3.2	6.53	0.03
	Synergy volume[4]	+++	++	+	++	±

[1]Combination index (CI) values for CalcuSyn are determined by testing fluoxazolevir with the other therapies at or near their EC_{50} values when tested independently.

[2]The synergy volume for CalcuSyn is defined as: +++ indicates strong synergy (CI < 0.7), ++ indicates moderate synergy (0.7 ≤ CI < 0.8), + indicates minor synergy (0.8 ≤ CI < 0.9) and ± indicates nearly additive (0.9 ≤ CI < 1.1).

[3]Log volume for MacSynergy II is determined by the volumes of the peaks and valleys of the synergy/antagonism surface plots.

[4]The synergy volume for MacSynergy II is defined as: +++ indicates strong synergy (log volume ≥ 9), ++ indicates moderate synergy (9 > log volume ≥ 5), + indicates minor synergy (5 > log volume ≥ 2) and ± indicates nearly additive (2 > log volume ≥ 0).

Table 2.

Pharmacokinetics of fluoxazolevir after 3 mg/kg IV and 10 mg/kg PO administration

Animal	CD-1 Mouse[1,2] (n=13, 3/time point)		SD Rat[1] (n=3)		Beagle Dog[1] (n=3)	
Route (Dose)	IV (3 mg/kg)	PO (10 mg/kg)	IV (3 mg/kg)	PO (10 mg/kg)	IV (3 mg/kg)	PO (10 mg/kg)
$AUC_{0-\infty}$[3] (μM•h)	0.871	1.15	6.47±4.17	0.268±0.041	1.59±0.13	0.753±0.179
$t_{1/2}$[3] (h)	24	37	17	19	29	19
T_{max}[3] (h)	-	2	-	0.3	-	0.8
C_{max}[3] (μM)	-	0.084	-	0.042±0.022	-	0.052±0.017
CLp[3] (mL/min/kg)	122	-	21±10	-	67±6	-
V_{dss}[3] (L/kg)	137	-	12±3	-	144±15	-
F[3] (%)	-	37	-	1.2	-	14

[1]The plasma concentration of fluoxazolevir was measured after a single dose of fluoxazolevir via PO or IV.

[2]Standard deviation could not be calculated since serial sampling was not performed with the mice. The three samples collected at each time point for the 13 mice were used only to define the overall pharmacokinetic profile.

[3]$AUC_{0-\infty}$: area under the curve from zero to infinity; $t_{1/2}$: half-life; T_{max}: time to reach the maximal concentration; C_{max}: maximal concentration after PO administration; CLp: clearance; V_{dss}: volume of distribution at steady-state; F: oral bioavailability.